HHS Public Access

Author manuscript

*Annu Rev Anal Chem (Palo Alto Calif)*. Author manuscript; available in PMC 2020 December 12.

Published in final edited form as:

*Annu Rev Anal Chem (Palo Alto Calif)*. 2020 June 12; 13(1): 17–43. doi:10.1146/annurev-anchem-090919-102205.

# Acoustic Microfluidics

**Peiran Zhang**[1], **Hunter Bachman**[1], **Adem Ozcelik**[2], **Tony Jun Huang**[1]

[1]Department of Mechanical Engineering and Materials Science, Duke University, Durham, North Carolina 27708, USA

[2]Department of Mechanical Engineering, Aydin Adnan Menderes University, Aydin 09010, Turkey

## Abstract

Acoustic microfluidic devices are powerful tools that use sound waves to manipulate micro- or nanoscale objects or fluids in analytical chemistry and biomedicine. Their simple device designs, biocompatible and contactless operation, and label-free nature are all characteristics that make acoustic microfluidic devices ideal platforms for fundamental research, diagnostics, and therapeutics. Herein, we summarize the physical principles underlying acoustic microfluidics and review their applications, with particular emphasis on the manipulation of macromolecules,cells,particles,model organisms, and fluidic flows.We also present future goals of this technology in analytical chemistry and biomedical research, as well as challenges and opportunities.

### Keywords

acoustics; lab-on-a-chip; analytical chemistry; single-cell analysis; liquid handling; model-organism manipulation

## 1. INTRODUCTION

Researchers have provided a continuous stream of developments in microfluidic technologies over the past several decades. These developments have continuously demonstrated the advantages of microfluidic methods with regard to the ability to manipulate micro- and nanoobjects and environments, such as cells, particles, organisms, or fluids with high precision, speed, and cost-effectiveness; these advantages are invaluable to an array of applications including in vitro diagnostic devices (1), high-throughput cell analysis (e.g., single-cell phenotyping) (2), and sample preparation (e.g., analyte separation, sequencing library construction) (3, 4).

On its challenging pathway toward the ultimate goal of micro total analysis systems (MicroTAS) or lab-on-a-chip, the field of microfluidics has been revolutionizing the ways in which samples within microsystems can be handled and manipulated; these micro- and

tony.huang@duke.edu.

DISCLOSURE STATEMENT

The authors are not aware of any affiliations, memberships, funding, or financial holdings that might be perceived as affecting the objectivity of this review.

nano-manipulations have been demonstrated via numerous methods, including electrics (5), magnetics (6), optics (7), plasmonics (8), acoustics, and hydrodynamics (9). Although all of these approaches have their unique advantages, each technique also presents disadvantages that hinder their practical use.

Acoustic-based microfluidics has been presented as a promising solution (10–14) for micro- and nanoscale manipulation. With an acoustic-based approach, researchers utilize gentle pressure waves to interact with microobjects and environments in a contactless and precise manner, enabling numerous chemical, biomedical, and industrial applications. And, although some features and capabilities of acoustic methods may overlap with optical, electrical, or magnetic platforms, acoustic microfluidic methods avoid some of these technologies' shortcomings to present the following useful advantages.

## Versatility

Acoustic microfluidic devices have six key factors that impart them with unprecedented versatility. The first of these factors is their unique ability to manipulate objects (e.g., cells and organisms) that range in size from nanometers to millimeters. Second, acoustic manipulation can be achieved with six degrees of freedom (i.e., translation and rotation along the *x*-, *y*-, *z*-axes) (14). Third, these devices have the ability to manipulate particles in a variety of fluid media (e.g., air, whole blood, or sputum), irrespective of the target particle's optical, magnetic, or electrical properties. Fourth, acoustic microfluidic devices offer the capability to manipulate particles within a fluid domain, as well as the fluid domain itself. Fifth, these devices have the ability to manipulate large groups of particles simultaneously, while also having the precision to control single particle motion. Lastly, acoustic microfluidic devices can operate at a wide range of fluidic throughputs, from nanoliter scale to tens of milliliters per minute.

## Biocompatibility

In acoustic microfluidics, target objects do not need to be physically in contact with other objects in order to achieve manipulation. This means minimal mechanical impacts and surface adsorption on solid surfaces as well as reduced heat conducted from the working transducers. In addition, acoustic microfluidics does not require specialized cocktail buffers or functional labels (e.g., magnetic nano-particles) for manipulation. Therefore, samples (e.g., cells and embryos) can be processed in their native fluids (e.g., blood, culture media, sea water) with minimal shocks from the analytic tool itself, maximizing the potential of maintaining the native states of the samples (15). Moreover, the majority of acoustic microfluidics devices employ relatively low acoustic powers (0.01–10 $W/cm^2$) and acoustic frequencies (1 kHz–500 MHz) comparable to ultrasonic imaging (2–18 MHz, <1 $W/cm^2$) (10, 14), which has been proven safe in prenatal diagnostics, implying the high level of biocompatibility of acoustic microfluidics. High biocompatibility of acoustic microfluidics was partially confirmed by recent studies (16, 17), which indicate that bioparticles such as zebrafish embryos placed in acoustic microfluidic devices for up to 33 min did not exhibit noticeable changes in viability or mortality rates.

### Precision

The propagation and interaction of acoustic waves in a microfluidic device can be applied in a highly controllable manner by spatial/temporal wave superposition to adapt into various microfluidic functions. The waves utilized in many acoustic microfluidic devices have wavelengths that are comparable to the sizes of many bioparticles, such as cells and vesicles, implying that acoustic microfluidic methods can manipulate particles or cells with high precision (resolution of ~1 μm).

### Flexibility

A wide variety of acoustic microfluidic mechanisms have been demonstrated, including acoustic streaming (18), acoustic radiation (19), acoustic dielectrophoresis (20), and acousto-thermal effect (21). The rich pool of fundamental physics involving acoustics and fluid mechanics allows the flexible design and implementation of versatile microfluidic functions by the best-suited pathway. In addition, acoustic microfluidics is very flexible in the choice of material used to fabricate the devices. For example, biocompatible or chemically compatible materials with good acoustic transparency can be chosen to make the device.

Compact and cost-effective nature: Compared to some other technologies, acoustic microfluidic technologies are relatively straightforward in their design. Transducers required in acoustic microfluidic operations are similar to designs used in commercial electronic applications (such as cell phones), making the devices inexpensive and reliable.

Convenient integration with other microfluidic technologies: Many acoustic microfluidic methods can be easily integrated with other microfluidic designs (e.g., hydrodynamic manipulation) to improve the functionality and level of control. This has enabled researchers to achieve even more impressive results relative to the technologies when used in isolation and suggests that these technologies can eventually be miniaturized and integrated with lab-on-a-chip devices (11).

Given these advantages, acoustic-based microfluidic methods have been gaining popularity in recent years. In this review, we summarize the principles behind and the technologies that enable acoustic microfluidics, discuss various applications of acoustic microfluidic technologies in analytical chemistry, biology, and medicine, and close with a discussion of the path forward for this technology.

## 2. OPERATING PRINCIPLES FOR ACOUSTIC MICROFLUIDICS

Generally,acoustic microfluidics can be described as the spatial and temporal manipulation of matter that is achieved when leveraging the exchange of energy between acoustic waves and solids, liquids, or gases. This section provides a brief introduction to the fundamental concepts behind acoustic microfluidic device design and operation, with emphasis on forces utilized during operation and examples of acoustic microfluidic systems that have been developed to produce and apply these forces.

### 2.1. Wave Generation and Propagation

Acoustic waves are mechanical vibrations that travel as disturbances in matter. One common method for generating an acoustic signal relies on the piezoelectric effect, which converts energy from an electrical signal into a mechanical disturbance (10). At the molecular level, the rearrangement of dipole moments in a piezoelectric material initiated by either an applied external electrical field or an induced mechanical stress generates mechanical deformations or an electric potential, respectively. Quartz is a natural material that demonstrates the piezoelectric phenomena; lead zirconate titanate (PZT) is an example of a material that does not show piezoelectric properties naturally, but it can be converted to a piezoelectric material after applying an external electric polarization. Friend & Yeo (10) provide a detailed review of piezoelectric materials and their applications. The vibration frequency of an acoustic transducer is determined by the frequency of the applied radio frequency signal; when the half-wavelength of the applied radio frequency signal matches the thickness of the piezoelectric crystal, the vibration amplitude becomes larger, which is known as the resonance condition (22). The vibrational mode of the transducers (e.g., thickness, shear, or lateral modes) is determined by either the crystal orientation or direction of electrical polarization (poling). In addition to the volumetric displacement of piezoelectric transducers, acoustic waves can also be generated along the surface of a piezoelectric material, such as lithium niobate ($LiNbO_3$), by using interlacing comb-finger-like electrode patterns called interdigitated transducers (IDTs) (11). When a radio frequency signal is applied to the IDTs, mechanical displacement of the substrate occurs along the interface; the resulting waveform is dependent upon the dimensions of the electrodes, the speed of sound in the material, input power of the applied electrical signal, and the design of the IDTs. For example, the equation $\upsilon/\lambda$ defines the frequency of a wave, where $\upsilon$ is the speed of sound in the substrate, and $\lambda$ represents the wavelength ($\lambda$ is equal to four times the electrode-to-electrode spacing of the IDTs). The two types of waves that are generated within the volume and along the surface of an elastic medium are generally referred to as bulk acoustic waves (BAWs) and surface acoustic waves (SAWs).

BAWs propagate through an elastic medium as a sinusoidal wave of crests and troughs, known as transverse or shear waves, and as a pattern of compressions and rarefactions, known as longitudinal or pressure waves. Transverse waves oscillate perpendicular to their propagation direction, whereas longitudinal waves oscillate along their propagation direction. SAWs have typical displacement amplitudes on the order of 10 Å and propagate along the interface of a piezoelectric surface before exponentially decaying into the substrate. Different forms of SAWs (e.g., Rayleigh, Lamb, or Scholte waves) that can propagate at the interfaces between solids, vacuums, and fluids can be excited by choosing complying crystal orientations and piezoelectric materials (10, 23). Rayleigh waves (24) are comprised of longitudinal and vertical shear components that can strongly couple with media on the propagation surface. Rayleigh waves are mostly used in SAW-based acoustic microfluidics where particles or cells are suspended in a liquid medium on the piezoelectric surface.

### 2.2. Acoustic Radiation Force and Acoustic Streaming

From a physics point of view, the manipulation of an object in a liquid medium by acoustic waves is achieved through the effect of acoustic radiation forces and acoustic streaming, which induce drag forces. Acoustic radiation forces and acoustic streaming are brought about by gradients in the acoustic field. These gradients arise due to phenomena such as scattering, absorption, reflection, and dampening that occur when the waves experience interference from fluids, channel structures, or particles and cells (25).

Acoustic radiation forces affect particles (beads,cells,bubbles,etc.) in a fluid by pushing or concentrating them. Acoustic radiation forces can be divided into primary and secondary radiation forces that act on single particles, or between particles, respectively (26). In a standing wave pattern, which is a superposition of two traveling acoustic waves, primary acoustic radiation forces directly move particles to pressure nodes or antinodes (27). Secondary acoustic radiation forces take advantage of interparticle forces and can be used to cluster particles. In-depth theoretical study of acoustic radiation forces for different cases can be found in the works of Doinikov (28) and Bruus (29). The primary acoustic radiation forces, $F_{RS}$, which act upon a compressible spherical object in a stationary acoustic field and inviscid fluid, are defined using the following equations (30):

$$F_{RS} = -\left(\frac{\pi p_0^2 V_p \beta_f}{2\lambda}\right)\phi(\beta,\rho)\sin\left(\frac{4\pi x}{\lambda}\right), \quad 1.$$

$$\phi(\beta,\rho) = \frac{5\rho_p - 2\rho_f}{2\rho_p + \rho_f} - \frac{\beta_p}{\beta_f}, \quad 2.$$

where $p_0$ and $V_p$ are the acoustic pressure and the volume of the particle, respectively; subscript $f$ and $p$ represent the fluid and particle, respectively (consistent in equations defined below); β, ρ, λ,and $x$ represent the compressibility [$\beta = 1/(\rho c^2)$], density, wavelength, and distance from a pressure node, respectively; lastly, ϕ represents the acoustic contrast factor, where the sign of the contrast factor determines the equilibrium positions of particles in the wave field.A positive acoustic contrast factor implies that particles equilibrate at pressure nodes and vice versa for particles with negative acoustic contrast factors. An important consideration for controlling the magnitude of the acoustic radiation forces is to have a large difference between the compressibility of the particles and the fluid medium. Particles or cells with varying properties (e.g., size or compressibility) will be affected differently by the acoustic field, which allows them to be separated. For example, when a mixture of spherical particles with diameters of 10,8,5,and 1 μm is introduced into a standing acoustic wave field (Figure 1a), the primary acoustic radiation force that acts on the larger particles is greater than the acoustic radiation force acting on the smaller particles (Figure 1b). As such, the larger particles would migrate to a pressure node more quickly (Figure 1a).

In addition to standing acoustic waves, traveling waves can also apply forces to suspended objects through wave scattering. The primary acoustic radiation force $F_{RT}$ acting on a

compressible spherical object in a traveling wave field and inviscid fluid is given by Equation 3 when $(k_f R)^2$ and $(k_p R)^2$ are negligible (31):

$$F_{RT} = \frac{3\pi R^6 \omega^4 P^2}{9\rho_f \left(2+\rho_f/\rho_p\right)^2 c_f{}^6}\left\{\left[3-\left(2+\frac{\rho_f}{\rho_p}\right)\frac{\rho_f c_f{}^2}{\rho_p c_p{}^2}\right]^2+2\left(1-\frac{\rho_f}{\rho_p}\right)^2\right\}. \quad 3.$$

Settnes & Bruus (32) developed Equation 4 to calculate the primary acoustic radiation force on compressible particles in traveling acoustic wave field and viscous fluid (i.e., $\delta_v$, $R \ll \lambda_s$),which is more relevant to the acoustophoresis applications in microchannels (31):

$$F_{RT} = \frac{3\pi R^3 \omega P^2}{\rho_f c_f{}^2}\left[\frac{\left(1-\frac{\rho_p}{\rho_f}\right)^2\left(1+\frac{\delta_v}{R}\right)\frac{\delta_v}{R}}{\left(1+2\frac{\rho_p}{\rho_f}\right)^2+9\left(1+2\frac{\rho_p}{\rho_f}\right)\frac{\delta_v}{R}+\frac{81}{2}\left(\frac{\delta_v{}^2}{R^2}+\frac{\delta_v{}^3}{R^3}+\frac{\delta_v{}^4}{2R^4}\right)}\right], \quad 4.$$

where $\delta_\upsilon$ is called viscous penetration depth ($\delta_\upsilon = \sqrt{2}v/\omega$), $\upsilon$ is the kinematic viscosity of the medium, $\omega$ is the angular frequency, and $k\,f$ and $kp$ are the wavenumbers in the medium and particle, respectively. Variables $P$, $R$, $\rho_f$, $\rho_p$, $c_f$, and $C_s$ are the acoustic pressure amplitude, scattering coefficient, densities, and sound speeds of the medium and the particle, respectively.

In addition to the acoustic radiation forces, acoustic streaming also plays an important role in the operation of acoustic microfluidic devices; acoustic streaming emerges due to an acoustic disturbance being attenuated within a viscous liquid medium. This streaming can manifest in many ways depending on the degree and procedure of attenuation (33). For instance, streaming due to an oscillating microbubble is called acoustic microstreaming, whereas streaming in a bulk fluid due to the attenuation of acoustic energy is called Eckart streaming. An important streaming mechanism in acoustic microfluidics is the boundary-driven acoustic streaming that arises from the rapid dissipation of the acoustic waves at solid boundaries. When determining the dominant force between acoustic radiation forces and the induced drag force from acoustic streaming, there is a threshold particle size above which acoustic radiation forces dominate (18). The hydrodynamic effect of acoustic streaming enables various fundamental fluidic functions such as mixing, pumping, particle concentration, and focusing (33). Details about the applications of these various mechanisms using acoustic streaming are presented by Wiklund et al. (33) and Sadhal (34).

### 2.3. Different Mechanisms for Acoustic Microfluidics—

Depending on their physical principles, acoustic microfluidic methods can be grouped into three major mechanistic categories: standing wave, traveling wave, or acoustic streaming (14). Various acoustic microfluidics technologies have been developed that are utilizing these physical principles. Some of the commonly used acoustic micromanipulation technologies are presented here.

**2.3.1. Acoustic resonators:** BAWs are used to form resonance modes, or eigenmodes, inside microchannels for manipulation of particles (35). A simple acoustic resonator is composed of an acoustic transducer, a hard-walled (e.g., glass or silicon) microchannel, and

an acoustic impedance matching layer between the two.A standing wave field forms due to the reflection of acoustic waves from the walls of the microchannel (or a reflector surface).Depending on the application,a desired number of pressure nodes and antinodes can be generated in the matching layer by adjusting the frequency (higher frequency yields a shorter wavelength and a larger number of nodes) (36). The trajectories and equilibrium states of the particles are governed by the acoustic radiation forces and the induced drag forces from acoustic streaming found within the resonators (37).For example,the variation in the acoustic radiation forces on particles with contrasting properties can be leveraged to separate differing particles in a continuous flow (38).

**2.3.2. Surface acoustic wave systems:** First explained by Lord Rayleigh (24), SAWs have been widely used in signal processing, sensing, and acoustic tweezing applications (11, 39). IDTs located on the surface of a piezoelectric surface are frequently used to generate SAWs with megahertz to gigahertz frequencies and with various wave fronts. The waves generated by IDTs on a piezoelectric surface are called traveling SAWs. Upon reaching a liquid domain, Rayleigh SAWs leak into and generate pressure fluctuations in the medium. Due to the difference between the velocity of sound in the solid substrate ($\upsilon_S$) and the liquid ($\upsilon_L$), longitudinal waves leak into the fluid at the Rayleigh angle ($\theta_R$), as defined by Snell's law, $sin(\theta_R) = \upsilon_L/\upsilon_S$. Interference between traveling SAWs can form standing SAWs that are characterized by linearly distributed pressure nodes and antinodes on the propagation surface or in a liquid media (11). Particles in the standing SAW field are drawn toward the nodes or antinodes depending on the sign of their acoustic contrast factors (2). The primary acoustic radiation force generated by the SAWs can be used to separate, sort, focus, and manipulate particles and cells either by a direct pushing effect or by moving the nodal positions through phase shift or frequency modulation in a standing SAW field (40).

**2.3.3. Acoustic bubble-based systems:** Microbubbles can be excited into oscillatory motion by an acoustic wave and can, in turn, generate acoustic radiation forces and acoustic microstreaming in a liquid medium (41). Leveraging acoustic radiation forces or streaming vortices generated by the oscillating bubbles, cells, particles, or small organisms can be trapped or circulated/rotated (42). The microstreaming vortices generated by the microbubbles also cause fluid motion that can be used to mix fluids moving at low Reynolds numbers in the channel (42, 43). As the bubble size decreases, the resonant frequency required to actuate the microbubbles increases (44). At the resonant frequency, a spherical microbubble undergoes radial oscillations, and at higher harmonics, the oscillation mode shape becomes more complex (18). Various geometries and shapes of the microstreaming flows are used in particle transport (45), fluid pumping (46), microswimmers (47) and for rotational manipulation of cells and microorganisms (18) in microchannels.

**2.3.4. Oscillating solid structures:** Oscillation of thin membranes and sharp-edged structures is used in fluid and droplet manipulation and rotational manipulation applications by implementing acoustic streaming effects (48). The sharp-edge structures or thin membranes oscillate similar to microbubbles, causing acoustic streaming; this acoustic streaming has been leveraged in fluid mixing, pumping, and microswimmer applications (48, 49). The oscillation frequency and amplitude of these structures are controlled by the

sharp-edge geometry, the frequency and amplitude of the applied signal, and the eigenmodes of the glass substrate.

**2.3.5. Transducer arrays and single beams:** Selective control of individual elements and the phase of the generated waveforms enables an array of acoustic transducers to produce novel acoustic beams that result in dexterous manipulation capabilities (50–52). For example, Foresti & Poulikakos (50) realized orbital motion and spinning of matter in air through individually controlling and peripherally positioning resonators (to modulate the node shapes and sizes of the acoustic field) such that asymmetric objects inside the acoustic field will levitate and experience a net rotational torque. Using a similar approach, 3D manipulation of particles is demonstrated by controlling the phase delay in a single-sided array of transducers (52). It is worth noting that these multielement acoustic systems require individual control of each transducer, which is costly for only manipulating of limited numbers of the objects over a large area of array.

**2.3.6. Complex beam formation: acoustic metamaterials and holograms:** Acoustic metamaterials enable modulation of acoustic waves in extraordinary ways, achieving unique capabilities such as subwavelength scale sound control and complex beam patterns (53–55). Based on these principles, localized control of the acoustic radiation forces via periodic phononic crystals is used in subwavelength manipulation and patterning of particles (56). Complex holographic patterns are also achieved using acoustic metamaterial unit cells and an iterative hologram generation algorithm to modulate the phase and the amplitude of the acoustic waves at each pixel (57).

## 3. MAJOR FUNCTIONALITIES OF ACOUSTIC MICROFLUIDIC TECHNOLOGIES

Following the introduction to the physical principals behind acoustic microfluidics and the basic device descriptions provided in the previous section, this portion presents a brief overview of ways in which acoustic waves are used to perform microfluidic functions.

### 3.1. Acoustic Patterning and Transportation

With SAW- and BAW-based acoustic microfluidic devices, samples with the characteristic sizes ranging from tens of nanometers (vesicles) to several millimeters (*Caenorhabditis elegans* and zebrafish) can be patterned and translated by acoustic waves in 1D to 3D spaces (58). For nanoparticles with distinct acoustic contrast with a medium (e.g., metal, diamond, silica), the lower size limit of particles that can be actuated is reduced to several nanometers with the interplay of acoustic-streaming-associated drag forces and acoustic radiation forces (59). Even for nanoscale analytes as small as enzymes, acoustic microfluidic devices can trigger the generation of coacervate droplet (e.g., PolyDADMAC) arrays using standing BAWs upon the vigorous mixing to sequester macromolar biomolecules as protocells (60). Besides particle patterning using ambient acoustic fields, patterning in selected regions is achieved by time-of-flight acoustic microfluidic devices based on the time-averaged superpositioning of two opposing nanosecond-scale pulses of SAWs to form localized, transient 1D standing SAW fields (19). To selectively manipulate small objects in 3D spaces,

holographic (52, 61) and digitalized (62, 63) acoustic levitation technologies were developed. Beyond the common well-established techniques described above, several interesting yet unconventional techniques have been developed as well. Zhou et al. (64) demonstrate the programmable transportation of sub-centimeter objects in arbitrary routes on the 2D plane by controlling nodal distribution of Chladni figures on a silicon wafer. Since the acoustic waves are applied in a contact-free manner and can be coupled to fluid containers, acoustic waves can be coupled into widely used, disposable petri dishes for cell patterning (65). Beyond the manipulation of spherical particles, the self-acoustophoretic nanowire motors have been realized based on the asymmetric response of acoustic radiations (66).

### 3.2. Acoustic Focusing

Cells or particles suspended and flowing through a microchannel that is aligned with a single pressure nodal line can be focused into a single-profile particle stream along the pressure node (67). In a cytometer configuration, particles are required to be aligned with and pass through the downstream laser detection point serially at high throughputs (e.g., ~3,500 events· $s^{-1}$) (67). Acoustic focusing eliminates the need for the sheath flows. Therefore, the focused bioparticles are not diluted and can remain in their native fluids, which minimizes the shocks from the buffer exchange or dilution. In practice, sheathless focusing using acoustic waves has been integrated with commercial acoustic focusing fluorescence cytometry (e.g., Attune NxT, Thermo Fisher Scientific) and stimulated Raman scattering cytometers (68).Additionally,parallel cell focusing has been demonstrated by aligning multiple nodal lines to the particle flow within the microchannel (69).

### 3.3. Acoustic Separation

Particles with different acoustic, mechanical, and hydrodynamic properties can be separated by acoustic streaming,traveling waves,standing waves,or a combination of the three mechanisms (70, 71). Acoustic separation has been rapidly gaining attention because of its excellent biocompatibility and label-free feature (15). Rare cells (15), bacteria (72), vesicles (3), and lipoproteins (73) with characteristic sizes ranging from 100 nm to 20 μm can be efficiently separated using acoustic microfluidics. For example, a 20-mL • $min^{-1}$ flow rate of platelet separation with an 88.9% red blood cell/white blood cell (RBC/WBC) removal rate has been demonstrated using quarter-wavelength resonators of BAWs (74). For nanoscale samples, a 4-μL · $min^{-1}$ flow rate can be achieved for separating exosomes from whole blood at a purity of ~98.4% using a 2-stage tilted-angle standing SAW device (3). Using traveling SAWs and a detachable microchannel, researchers were able to separate 98% of the 10-μm particles from 15-μm particles (75). Furthermore, cellular subsets (e.g., RBCs, WBCs, platelets) in whole blood can be trapped and separated from other components by the localized acoustic vortices generated by the oscillation of air bubbles along the side wall of microchannels (71). Besides label-free separation, cells also can be linked with antibody-conjugated acoustic markers [e.g., polydimethylsiloxane, PDMS beads (76), air bubbles (77)] to enable high-efficiency and multichannel separation.

### 3.4. Acoustic Sorting

Different from particle separation, the sorting function involves active actuation of single particles gated by an upstream detection unit with feedback control. To avoid unexpected actuation on the adjacent particles in the single-profile particle stream, the acoustic waves need to be focused into a narrow beam with high intensity for robust particle actuation. Recently, 3,500 event $\cdot s^{-1}$ cell detection and sorting throughput has been achieved using focused standing SAW beams with widths of 120 μm and a duration of 100 μs (67). The width of the focusing beam can be further narrowed down to 25 μm by reducing the wavelength of the SAW (78).Acoustic waveguides are employed to confine traveling waves locally in the microchannel and have achieved 330-μs deflection duration for particle/droplet sorting (79).Besides sorting based on acoustic radiation forces,several successful attempts on particle/droplet sorting using acoustic streaming and acousto-thermal Marangoni effects have also been reported (21).

### 3.5. Acoustic Enrichment and Micro- or Nanoassembly

Micro- or nanoscale particles can be concentrated in a standing acoustic field. In general, concentrated cell suspensions in standing acoustic wave fields can be assembled into linear or spheroid-like clusters (80). Apart from conventional acoustic enrichment methods based on standing waves and traveling waves (80, 81), there are also several unconventional approaches. For example, submicron-scale particles can be attracted to the vicinity of microscale seeding particles due to the secondary scattering and the associated size exclusion effect of particle clusters (82). Boundary layer streaming in an acoustic field has been demonstrated to concentrate latex nanoparticles with a comparable dimension of the thickness of boundary layer at the antinodes (83). Localized acoustic streaming vortices can also be utilized to concentrate nanoscale particles using gigahertz or terahertz transducers (84). Sung and coworkers (85) demonstrated that particles with different sizes inside an open drop rotated by a SAW will be concentrated in different regions inside the droplet, which can be tuned by varying the dimension of droplet and the acoustic wavelengths through critical values. Yeo's group (86) demonstrated the combined effect of turbulent convective mixing in an evaporating droplet, and the acoustoelectric coupling on the $LiNbO_3$ substrate, which could uniformly assemble nanometal-organic frameworks in oriented stacking of monolayers.

### 3.6. Acoustic-Based Orientational Control

Acoustic streaming vortices can be generated upon the interaction of fluids with acoustic waves or oscillating boundaries. Cells, particle clusters, and model organisms can be stabilized by the acoustic streaming vortices and be rotated at a resolution of 4° (18, 87). In contrast, the horizontal orientation of nonspherical objects (e.g., cell clusters, *C. elegans*) can be precisely tuned by reshaping the Gor'kov potential wells upon dynamic wave superposition (88). Neild and colleagues (89) also demonstrated the orientation control of an array of single nonspherical cells (e.g., RBCs) using a 2D standing SAW with a characteristic half-wavelength comparable to the size of cells.

### 3.7. Acoustic-Based Fluid Actuation

Acoustic streaming has been widely explored for fluid jetting, pumping, or mixing in various formats of fluid containers, including microfluidic chips (48, 90, 91), open substrates (92, 93), and multiwell plates (94). The steady flow of acoustic streaming can be generated on demand by either oscillating boundaries or the attenuation of high-frequency acoustic waves in a viscous fluid for various engineering purposes. Liquid droplets can be translated in a contact-free manner by either holographic (52,61) or digital acoustic levitation (62,63) in a 3D space with millimeter-level resolution. Recently, there has been an attempt using acoustic streaming–induced hydrodynamic traps to translate, merge, split, and mix droplets floating on the surface of a denser oil layer for reaction automation (95). In droplet microfluidics, SAW devices have demonstrated various droplet operations involving trapping (96), mixing, sorting (79), dispensing (97), in-droplet focusing (98), and splitting (99). For droplet dispensing, acoustic droplet ejection (e.g., Echo 555, Labcyte Inc.) enables nozzleless, pico- or nanoliter droplet dispensing at kilohertz speeds (100, 101). Another dispensing method actively regulates the detachment of liquid flowing through a nozzle, allowing the robust dispensing of liquids (102). Submicron or micron aerosol droplets can also be generated from bulk liquid using acoustic atomization (103). Miansari & Friend (104) demonstrate the translation of a femtoliter droplet through a nanoslit involving the interplay of acoustic radiation and capillary pressure. When manipulating oil droplets on a SAW substrate, the oil film will coun-terintuitively extend toward the opposite direction of SAW propagation due to transverse Fresnel diffraction (i.e., acoustic wetting) (105).

### 3.8. Acoustic Cavitation

Applying high-intensity focused ultrasound (HIFU) beams in liquids causes cavitation bubbles to form and oscillate at the focal point (106); at the same time, a heating effect from the concentrated acoustic signal decreases the solubility of dissolved gas, leading to further bubble aggregation (106). The vigorous oscillation of the air–liquid boundary under high-amplitude pressure fluctuation at the acoustic focal point induces strong acoustic streaming and can disrupt the structures of cells and tissues in the vicinity (107), the effect of which is used for in situ sonoporation for intercellular delivery or cell lysis (108).

### 3.9. Acoustic-Based Sensing

BAW resonators, including quartz crystal microbalances (109), thin-film bulk acoustic resonators (110), and solidly mounted resonators (111), have been used for sensing at extremely high sensitivities (femtograms to picograms) of surface mass loading. Love waves can be used to detect the binding of analytes due to a shift in the resonant frequency caused by mass loading in the region of wave propagation (112).

### 3.10. Acoustic-Based Biophysical Measurements

For biophysical measurements, several parameters including the compressibility (113) and acoustic impedance (81) of single cells or *C.elegans* (114) in acoustic fields can be measured by analyzing particle trajectory and tracking the equilibrium position. Suspended microchannel resonators are sensitive enough to profile the mass growth of single cells by recoding the time-resolved shifts of resonant frequency (115). Furthermore, the binding

force (piconewton-level) between two biomacromolecules attached on an actuation particle or substrate can be quantitatively characterized by acoustic force spectroscopy (116).

### 3.11. Acoustic-Based Heating

Besides physical manipulation and sensing, acoustic waves can be used in rapid heating of targeted areas via viscous attenuation of high-frequency acoustic waves. Isothermal polymerase chain reactions (PCRs) have been demonstrated using acoustic heating in an oil-covered droplet (93). Acousto-thermal Marangoni flows can be generated on demand locally in a microchannel and used to deflect moving droplets (21).

## 4. REPRESENTATIVE APPLICATIONS OF ACOUSTIC MICROFLUIDICS

The preceding descriptions provide details on the various acoustic microfluidic methods that researchers have used to achieve complex manipulations. This section provides several examples of unique applications in which the previously described methods have been utilized. Table 1 shows the contactless, label-free, and biocompatible manipulation of various biosamples ranging from macromolecules, cells, and tissues to model organisms enabled by acoustic microfluidics.

### 4.1. Processing of Nanoscale Analytes

Concentration, separation, sorting, patterning, and generation of nanoscale analytes with diagnostic or therapeutic value (e.g., exosomes, macro-biomolecules) have long been a pursuit in the acoustic microfluidics community. As the particle size scales down, phenomena involving Brownian motion,electrokinetics,capillary actuation,and viscous drag will become significant,leading to distinct strategies for manipulating nanoscale analytes compared with micro-manipulation using acoustic waves.

**4.1.1. Nanoparticle concentration—**Acoustic microfluidics has enabled the visualization and isolation of nanoparticles across a variety of particle sizes. For example, Collins et al. (128) used high-frequency (~200–600 MHz), highly focused traveling SAWs to trap nanoparticles using size exclusion. In this work, the authors used a combination of acoustic radiation and acoustic streaming effects to trap and concentrate nanoparticles with sizes down to 300 nm. Whitehill et al. (129) used low frequencies (~200 Hz) to manipulate nanoparticles in droplets. This work also used the effects of acoustic radiation and acoustic streaming and was able to manipulate 190-nm nanoparticles into a concentric ring within a droplet. Mao et al. (130) used SAWs (~4MHz)andaglass capillary to concentrate nanoparticles ranging in size from 80 to 500 nm. Acoustic streaming generated by the SAWs concentrated particles at the center of the channel, enhancing the signal emitted by fluorescently labeled nanocomplexes.

**4.1.2. Nanoparticle separation—**Nanosized biological samples have been shown to contain critical information for both diagnostic and therapeutic efforts. However, the isolation and separation of these samples have hindered their use in practical medical scenarios. As such, researchers have sought to use acoustic microfluidic methods to isolate these samples. Sehgal & Kirby (131) utilized SAWs and a Fabry-Perot-type resonator to

separate 100- and 300-nm nanoparticles in a continuous flow (Figure 2a–c). Wu et al. (132) utilized a tilted-angle standing SAW to increase separation differences between dissimilarly sized particles; the authors used this increased separation distance to separate 110- and 500-nm particles. Advancing this work, the team combined two acoustic separation units to separate exosomes from whole blood samples (3). The authors first separated out large blood cells above 1 μm in size using the first acoustic separation unit; they then removed all particles greater than 140 nm to isolate the exosomes using the second acoustic separation unit. However, this size-based separation meant that contaminates, such as lipo-proteins, remained in the collection with the exosomes. In order to rectify this, the group developed a separation module that relied on particles' acoustic contrast factor to achieve separation (73); the opposite contrast factors of the exosomes and proteins meant that a purer exosome sample could be created. Submicron particle separation has also been demonstrated using the boundary layer acoustic streaming on cantilevers (83).

**4.1.3. Nanomaterial patterning, alignment, and generation—**Researchers have shown the potential benefits of nanoparticles and nanomaterials in electronics, optics, and biomedicine, but the generation and manipulation of these particles still present challenges. Tang et al. (133) generated functional liquid metal nanoparticles using a vapor cavity–generating ultrasonic system. The particles generated in this work had a relatively narrow size distribution relative to those in previously reported studies and produced nanoparticles approximately 200 nm in size. Yunus et al. (20) used an array of bulk transducers to pattern conductive nanoparticles for the generation of embedded and electrically connected arrays (Figure 2d). This work was used to generate 3D structures for embedded electronics applications (Figure 2e). Smorodin et al. (134) used SAWs to align single-walled carbon nanotubes onto prepatterned gold electrodes. The alignment of single-walled nanotubes into a prescribed pattern is the first step in leveraging their unique properties.

**4.1.4. Nanofluidics—**One of the many benefits of microfluidic technologies is the relatively low sample volume requirements.From a biological and chemical perspective,this is extremely helpful, owing to the fact that small sample volumes can reduce both the use of expensive reagents and reaction times. Although these benefits have been explored and leveraged in many applications, researchers still attempt to manipulate even smaller volumes of fluids, down to the nanoliter and picoliter levels. Miansari & Friend (104) explored the use of SAWs to manipulate small volumes of fluids in capillaries. This process was used to achieve pumpless size exclusion separation and even control droplets as small as 10 fL.

### 4.2. Single-Cell Manipulation and Analysis

Single-cell analysis can reveal the underlying heterogeneity, kinetics, and rare events masked by the bulk culture. Acoustic microfluidics aims to manipulate single cells based on their acousto-mechanical or hydrodynamic properties with high precision, flexibility, and unprecedented biocompatibility.

**4.2.1. Single-cell biophysical measurements—**Acoustic microfluidics allows contact-free, biocompatible biophysical measurements on living single cells with unprecedented speed and precision. For example, suspended microchannel resonators

employ a microfabricated cantilever with a U-shaped microfluidic channel (Figure 3a–d) (115). Based on a shift in the resonant frequency as the analyte particles flow through the channel, the mass, density, and volume of single cells can be measured by the device (115, 135). Using this approach, high-throughput (i.e., 60 cells/h) monitoring of the mass growth of single bacterial cells is achieved by flowing a diluted cell suspension through an array of sensors integrated with time-delay channels (115). A single cell in the flowing suspension can be specifically identified using probabilistic modeling with the robust demonstration of continuous monitoring of cell growth over 3 h (115). The stiffness of the cells can also be determined by analyzing the size-normalized acoustic scattering of single cells, with a resolution of deformation of 15 nm (135). Using this mechanism, researchers profiled the dynamic stiffness change (over a 4-h period) during the mitosis of single L1210 cells (135). This approach resolved the mass of a 150-nm gold nanoparticle (i.e., ~30 fg) at an uncertainty level of 41 attograms (136). Recently, the resolution was reduced to as low as 27 attograms, bringing the precision of mass measurement to an unprecedented level (137). With the ultrasensitivity of the detection of mass loading, the binding of biomolecules can be detected with a resolution of $1.4 \times 10^{-8}$ ng · $\mu m^{-2}$ for biotinylated bovine serum albumin (BSA) (138).

The kinetics of cell trapping in a standing acoustic wave field correlates to the acousto-mechanical properties of the cells based on the force balance of acoustic radiation and viscous drag (113). Using a reference particle with known density, diameter, and mass, the acoustic energy density $E_{ac}$ of the standing acoustic wave field becomes a known parameter (113). Thus, based on the reasonable estimation of cell volume and density, analysis of the kinetics of cell trajectories can lead to the determination of the compressibility of single cells (113). This method has evolved to the flow-mode measurement of acoustic contrast factor at a throughput of 600 cell · $min^{-1}$ (139). Voldman and coworkers (2) used a unique method to phenotype the acoustic impedances of single cells by analyzing their equilibrium position in a standing wave field with acoustic contrast gradient (i.e., iodixanol), providing further insight that fluorescent cytometry is not capable of achieving. Acoustic force spectroscopy uses extremely well-calibrated acoustic fields to levitate an actuation particle near the bottom of the channel (116). Single-molecule pair binding can be profiled with piconewton-level resolution by measuring the kinetics of positional shifts between the bead and surface, which are covalently bonded to the molecules (116). An interesting attempt to profile the size of single cells used 375-MHz focused ultrasonic beams and analyzed the scattered signals like optical cytometers (140). Single cells can be deformed using focused ultrasound beams to characterize the stiffness of cancer cells (141). Researchers have also attempted to use a piezoelectric inkjet to eject single cell droplets with the goal of integrating mass spectroscopy to provide a label-free method for profiling cellular composition with unprecedented resolution for differentiating subpopulations of cells (142).

**4.2.2. Single-cell manipulation and stimulation—**As the wavelength of acoustic beams is scaled down to dimensions comparable to the size of single cells or particles, acoustic microfluidic devices can enable direct manipulation in a contact-free and biocompatible manner (14). Single-cell sonoporation employs well-controlled cavitation bubbles to gently disrupt the membrane of single cells for the targeted delivery of DNA,

RNA, or drugs in a nondestructive manner (108). This technique has been demonstrated in combination with membrane clamps to profile short-term cellular responses (108). The Neild lab (89) demonstrated the patterning and orientation control of single-cell arrays using acoustic tweezers with characteristic wavelengths comparable to the size of single cells with negligible influence on the cell viability at low input powers. The single cells in an array were held in position while changing the medium (89). Huang and colleagues (143) demonstrated precise control over the distance between two single cells when using acoustic tweezers to study cell–cell interactions (i.e., gap junction–based dye transfer). In a similar device configuration, the trapped single cells can be levitated by utilizing the 3D acoustic streaming at the pressure node and precisely placed at arbitrary positions when the acoustic field is off, providing a unique strategy for single-cell printing (Figure 3e–g) (144). Similar to acoustic holograms (55),single-beam acoustic tweezers based on swirling Rayleigh wave synthesis (i.e.,spiraling shaped interdigital transducers) can couple single traps in fluid chambers for single-particle (i.e., 30-μm polystyrene bead) manipulation (145). In the acoustic droplet ejection configuration, the on-demand, probabilistic encapsulation of single cells into extracellular matrix gels with 89.8% viability was demonstrated (146).

### 4.3. Manipulation of Model Organisms

Model organisms are essential tools for biomedicine and analytical chemistry to study complex biological process, high-throughput compound screening, and pharmacokinetic modeling at the system level. Chalasani and colleagues (122) demonstrated a contact-free, noninvasive technique for activating ultrasonically sensitized neurons in the *C. elegans* nematode (i.e., sonogenetics) by using a gentle ultrasound beam and specially engineered microbubbles to enhance oscillation and robustness (Figure 4a,b). Zheng and coworkers (121) showed that the mechanical effects of short-pulsed SAWs (28.11 MHz) can evoke ASH (a polymodal sensory neuron) of *C. elegans* without significant impact on AFD (a thermal-sensitive neuron). Ding et al. (58) reported the translation, orientation, and stretching of *C. elegans*.

The rotational control of *C. elegans* is achieved using the localized acoustic streaming vortices near the oscillating bubble array on the side wall of the microchannel with a resolution of 4° to visualize the 3D neural nodes and networks of the worm (18). Zhang et al. (87) applied unbalanced standing SAWs to the microchannel 0.75 wavelengths in width to induce acoustic streaming vortices for worm rotation. Neurons, axons, dendrites, and vulval muscles can be visualized in the rotational view. Similar to the compressibility measure of single cells, the acoustic compressibility of living *C. elegans* can also be estimated by analyzing the trajectories of the worm in the standing acoustic wave field together with calibration particles (114). The combination of light sheet microscopy and contactless sample confinement using acoustic microfluidics provides a unique advantage: real-time control of the sample due to the elimination of gels that limit the diffusion speed of environmental stimuli and interfere with the development of embryos (123). Leveraging this advantage, researchers imaged the embryos of *Danio rerio*, ripe *Branchiostoma lanceolatum*,and *Ciona intestinalis* and analyzed the cardiac cycles of zebrafish larvae (Figure 4c–g) (123). Previous studies indicate that acoustic levitation of zebrafish embryos (<2,000 s) does not interfere with their development process (16).

### 4.4. Liquid Handling for Bioassays

Bioassays involve the manipulation of liquids in various formats (e.g., whole blood, sputum, stool, honey, and emulsions). Acoustic microfluidics allows label-free, high-throughput, and biocompatible automated liquid handling and cell separation, even for complex clinical samples.

**4.4.1. Droplet manipulation—**Various contact-free liquid handling techniques have been developed for automating high-throughput reactions in laboratories. Acoustic levitation pioneers contactless liquid handling by suspending droplets using standing waves in air (147) and has evolved to either holographic (61) or digital (50) manipulation of droplets over an array of transducers. Poulikakos and coworkers (62) designed an acoustic reflector-resonator array for the digitalized, contact-free transportation of cells and transfection reagents in droplets floating in air (Figure 5a–c). Ferrari's group (63) demonstrated contact-free droplet merging and dispensing into multiwell plates using gravity for transfection and implementing an inverted digitalized air reflector-resonator array. The Huang lab (95) developed a contactless acoustic streaming–based droplet manipulation technique (i.e., digital acoustofluidics) that moves aqueous droplets floating on the surface of a dense fluorinert oil to enable cascade enzymatic reactions. Various other acoustic liquid–dispensing techniques have also demonstrated great potential in reaction automation for high-throughput screening. For nozzleless acoustic droplet ejection, BAW transducers [e.g., (148) and Echo 555, Labcyte Inc.], IDTs (100), and air reflector lenses (101) have been successfully demonstrated for on-demand droplet ejection with varied types of fluids (water, photoresists), tunable volumes (picoliters to microliters per drop), throughputs (up to several kilohertz), and directions (~27.5° with respect to the vertical axis). Acoustophoretic printing utilizes the acoustophoretic forces generated by Fabry-Perot resonators to regulate the detachment of liquids flowing through a nozzle. This provides a unique versatility of liquid choices with a wide range of $Z$ numbers (the inverse of an Ohnesorge number), including viscous honey, UV resists, bioinks, water, and even liquid metal (102).

**4.4.2. Actuation of fluids on chip—**Acoustic-induced streaming flows have been used for liquid pumping in various chip-based applications. Based on this mechanism, Sesen et al. (149) reported a SAW-activated on-chip programmable pipette (Figure 5d–f ) that could sample from monodisperse droplets upon the negative pressure induced by pumping oil. A simple approach for fluid pumping was demonstrated using traveling SAWs and straight microchannels to drive fluid motion (90). Furthermore, Langelier et al. (150) realized a 4-channel, individually addressable pump by applying multifrequency signals to the tuned acoustic resonator array.

**4.4.3. Preparation of clinical liquid samples—**Huang et al. (91) developed an acoustofluidic microvortex mixer that produced sufficient streaming to homogenize viscous sputum samples with the redox reagent dithiothreitol. More recently, Zhao et al. (151) modified the sputum liquefaction design to liquefy stool samples and used the platform to investigate bacterial presence in complex biosamples. Dealing with whole blood in microfluidic devices can be challenging owing to its increased viscosity and high cell concentration. In this regard, Petersson et al. (152) developed a simple acoustic microfluidic

resonator capable of measuring hematocrit from whole blood within 60 s. The Cooper lab (93) demonstrated that concentric acoustic streaming vortices inside a droplet induced by unbalanced ultrasonic waves can be used for the concentration and lysis of red blood cells and the subsequent thermocycling for downstream molecular diagnosis.

### 4.5. Isolating Rare Cells from Patient Samples

The isolation and identification of rare cells in biofluids contribute to clinical diagnoses and therapy. Li et al. (15) used a unique tilted-angle standing SAW field to separate circulating tumor cells (CTCs, 1–100 cells/mL) from WBCs with a recovery rate of greater than 83%. Wu et al. (153) improved on this device's performance by increasing the throughput from 20 to 125 μL/min. Recently, Liu et al. (154) used coated microbeads to increase the acoustic radiation force, which helped to distinguish the CTCs from blood cells for SAW separation. Antfolk et al. (124) used a BAW transducer to separate breast cancer cells that had been spiked into WBCs with an efficiency of greater than 90%.

### 4.6. Tissue Engineering

Acoustic patterning has been presented as a potential pathway for researchers to develop and culture these cellular networks. For example, Nguyen et al. (155) used standing SAWs to achieve 3D patterning of microparticles into a 3D matrix. Bouyer et al. (119) used a similar principle, with BAW transducers to achieve 3D patterning of neuroprogenitor stem cells, which were cultured into an interconnected network of neuron cells. The acoustically patterned gel with cells can be in vivo cultured on living mice for damage recovery (i.e.,28 days) with promising compatibility (120).

## 5. CONCLUSIONS AND PERSPECTIVES

Acoustic microfluidics has been successfully applied to a variety of important applications in analytical chemistry and biomedicine, including cell separation, cell patterning, cell lysis, sample enrichment, fluid pumping, reagent mixing, on-chip PCR, biophysical measurements, and manipulation of model organisms. These applications mimic the functions of a plethora of equipment found in a typical laboratory, suggesting that these microsystems could replace conventional tools. However, many technical hurdles need to be overcome, including unlocking the ability to manipulate particles <100 nm in size. Current limitations with regard to the wavelength and diffraction limits of acoustic manipulation methods have prevented this achievement. In addition, researchers must work to improve the translational resolution for particle and cell manipulation to submicron levels, while improving the resolution for rotational manipulation to single-degree accuracy. The robustness of acoustic microfluidic methods' six-axis particle control must also be improved. That is, although current methods may provide excellent control in planar translation, *z*-axis manipulation lacks the same dexterity and presents a future challenge.

Regarding cell and particle patterning, most of the current acoustic microfluidic methods are confined to forming prescribed geometric patterns defined by orderly standing wave fields. To have more practicality in bioengineering applications, including tissue engineering, researchers need to achieve arbitrary cell patterning in any desired shape. Similarly, current

acoustic-based methods lack the ability to selectively control one cell or particle within a field of many. Techniques involving acoustic metamaterials, metasurfaces, or holograms could potentially provide the pathway for overcoming the roadblocks associated with complex manipulations of acoustic fields and the objects within them, achieving arbitrary and selective cell manipulation and patterning.

In addition, on the whole, acoustic microfluidic tools have only been demonstrated as discrete components or functions within a lab-on-a-chip platform; additionally, many of the tools developed still require extensive background knowledge and expensive equipment to operate. In order to facilitate the increased adoption of acoustic microfluidics by researchers, it is necessary to build user-friendly, turnkey, integrated devices that perform conventional laboratory processes with minimal specialized training. Similar to how software collaborations formed the open-source coding model, researchers can achieve this goal by combining proven, discrete acoustic microfluidic designs with each other, or integrating other lab-on-a-chip units, into a single device. In order to complete these systems, function generators, amplifiers, acoustic transducers, and signal processors must be incorporated as well. Toward this goal, researchers have recently begun developing portable acoustic microfluidic tools that attempt to bridge the gap between developmental stages and end use. Most of these platforms attempt to use commercial products, such as cell phones/media players or open source control systems to circumvent much of the technology needed for traditional acoustic microfluidic device operation. Although these are good first steps, more work is needed to improve the desirability and adoption of acoustic microfluidic solutions to biomedical endeavors. It is our hope that through continued focus, researchers will develop the accessories and adaptations necessary to bring the benefits of acoustic microfluidic technology to a broader audience.

## ACKNOWLEDGMENTS

This research was supported by the US National Institutes of Health (R01GM132603, UG3TR002978, R01HD086325, R33CA223908, and R01GM127714) and the US Army Medical Research Acquisition Activity (W81XWH-18–1-0242).

## LITERATURE CITED

1. Chin CD, Linder V, Sia SK. 2012 Commercialization of microfluidic point-of-care diagnostic devices. Lab Chip 12(12):2118–34 [PubMed: 22344520]
2. Augustsson P, Karlsen JT, Su HW, Bruus H, Voldman J. 2016 Iso-acoustic focusing of cells for size-insensitive acousto-mechanical phenotyping. Nat. Commun. 7:11556 [PubMed: 27180912]
3. Wu M, Ouyang Y, Wang Z, Zhang R, Huang P-H, et al. 2017 Isolation of exosomes from whole blood by integrating acoustics and microfluidics. PNAS 114(40):10584–89 [PubMed: 28923936]
4. Klein A, Mazutis L, Akartuna I, Tallapragada N, Veres A, et al. 2015 Droplet barcoding for single-cell transcriptomics applied to embryonic stem cells. Cell 161(5):1187–201 [PubMed: 26000487]
5. Sidelman N, Cohen M, Kolbe A, Zalevsky Z, Herrman A, Richter S. 2015 Rapid particle patterning in surface deposited micro-droplets of low ionic content via low-voltage electrochemistry and electrokinetics. Sci. Rep. 5(1):13095 [PubMed: 26293477]
6. Lebel P, Basu A, Oberstrass FC, Tretter EM, Bryant Z. 2014 Gold rotor bead tracking for high-speed measurements of DNA twist, torque and extension. Nat. Methods 11(4):456–62 [PubMed: 24562422]

7. Fan X, White IM. 2011 Optofluidic microsystems for chemical and biological analysis. Nat. Photon. 5(10):591–97
8. Wang K, Schonbrun E, Steinvurzel P, Crozier KB. 2011 Trapping and rotating nanoparticles using a plasmonic nano-tweezer with an integrated heat sink. Nat. Commun. 2(1):469 [PubMed: 21915111]
9. Kessler JO. 1985 Hydrodynamic focusing of motile algal cells. Nature 313(5999):218–20
10. Friend J, Yeo LY. 2011 Microscale acoustofluidics: microfluidics driven via acoustics and ultrasonics. Rev. Mod. Phys. 83(2):647–704
11. Ding X, Li P, Lin SCS, Stratton ZS, Nama N, et al. 2013 Surface acoustic wave microfluidics. Lab Chip 13(18):3626–49 [PubMed: 23900527]
12. Fu YQ, Luo JK, Du XY, Flewitt AJ, Li Y, et al. 2010 Recent developments on ZnO films for acoustic wave based bio-sensing and microfluidic applications: a review. Sens. Actuators B Chem. 143(2):606–19
13. Yeo LY, Friend JR. 2014 Surface acoustic wave microfluidics. Annu. Rev. Fluid Mech. 46:379–406
14. Ozcelik A, Rufo J, Guo F, Gu Y, Li P, et al. 2018 Acoustic tweezers for the life sciences. Nat. Methods 15(12):1021–28 [PubMed: 30478321]
15. Li P, Mao Z, Peng Z, Zhou L, Chen Y, et al. 2015 Acoustic separation of circulating tumor cells. PNAS 112(16):4970–75 [PubMed: 25848039]
16. Sundvik M, Nieminen HJ, Salmi A, Panula P, Hæggström E. 2015 Effects of acoustic levitation on the development of zebrafish, *Danio rerio*, embryos. Sci. Rep. 5(1):13596 [PubMed: 26337364]
17. Lam KH, Li Y, Li Y, Lim HG, Zhou Q, Shung KK. 2016 Multifunctional single beam acoustic tweezer for non-invasive cell/organism manipulation and tissue imaging. Sci. Rep. 6:37554 [PubMed: 27874052]
18. Ahmed D, Ozcelik A, Bojanala N, Nama N, Upadhyay A, et al. 2016 Rotational manipulation of single cells and organisms using acoustic waves. Nat. Commun. 7:11085 [PubMed: 27004764]
19. Collins DJ, Devendran C, Ma Z, Ng JW, Neild A, Ai Y. 2016 Acoustic tweezers via sub-time-of-flight regime surface acoustic waves. Sci. Adv 2(7):e1600089 [PubMed: 27453940]
20. Yunus DE, Sohrabi S, He R, Shi W, Liu Y. 2017 Acoustic patterning for 3D embedded electrically conductive wire in stereolithography. J. Micromech. Microeng 27(4):045016 [PubMed: 30344375]
21. Park J, Jung JH, Destgeer G, Ahmed H, Park K, Sung HJ. 2017 Acoustothermal tweezer for droplet sorting in a disposable microfluidic chip. Lab Chip 17(6):1031–40 [PubMed: 28243644]
22. Dual J, Hahn P, Leibacher I, Möller D, Schwarz T. 2012 Acoustofluidics 6: experimental characterization of ultrasonic particle manipulation devices. Lab Chip 12(5):852–62 [PubMed: 22301707]
23. Gedge M, Hill M. 2012 Acoustofluidics 17: theory and applications of surface acoustic wave devices for particle manipulation. Lab Chip 12(17):2998–3007 [PubMed: 22842855]
24. Rayleigh L. 1885 On waves propagated along the plane surface of an elastic solid. Proc. Lond. Math. Soc s-17(1):4–11
25. Sarvazyan AP, Rudenko OV, Nyborg WL. 2010 Biomedical applications of radiation force of ultrasound: historical roots and physical basis. Ultrasound Med. Biol. 36(9):1379–94 [PubMed: 20800165]
26. Hahn P, Leibacher I, Baasch T, Dual J. 2015 Numerical simulation of acoustofluidic manipulation by radiation forces and acoustic streaming for complex particles. Lab Chip 15(22):4302–13 [PubMed: 26448531]
27. Shi J, Huang H, Stratton Z, Huang Y, Huang TJ. 2009 Continuous particle separation in a microfluidic channel via standing surface acoustic waves (SSAW). Lab Chip 9(23):3354–59 [PubMed: 19904400]
28. Doinikov AA. 1996 Theory of acoustic radiation pressure for actual fluids. Phys. Rev. E 54(6):6297–303
29. Bruus H. 2012 Acoustofluidics 7: the acoustic radiation force on small particles. Lab Chip 12(6):1014–21 [PubMed: 22349937]
30. Yosioka K,Kawasima Y.1955Acoustic radiation pressure on a compressible sphere. Acta Acust.5(3):167–73

31. Johnson KA, Vormohr HR, Doinikov AA, Bouakaz A, Shields CW, et al. 2016 Experimental verification of theoretical equations for acoustic radiation force on compressible spherical particles in traveling waves. Phys. Rev. E 93(5):053109 [PubMed: 27300980]
32. Settnes M, Bruus H. 2012 Forces acting on a small particle in an acoustical field in a viscous fluid. Phys. Rev. E 85:016327
33. Wiklund M,Green R,Ohlin M.2012Acoustofluidics 14: applications of acoustic streaming in microfluidic devices. Lab Chip 12(14):2438–51 [PubMed: 22688253]
34. Sadhal SS. 2012 Acoustofluidics 13: analysis of acoustic streaming by perturbation methods. Lab Chip 12(13):2292–300 [PubMed: 22660643]
35. Bruus H. 2012 Acoustofluidics 2: perturbation theory and ultrasound resonance modes. Lab Chip 12(1):20–28 [PubMed: 22105715]
36. Lenshof A, Evander M, Laurell T, Nilsson J. 2012 Acoustofluidics 5: building microfluidic acoustic resonators. Lab Chip 12(4):684–95 [PubMed: 22246532]
37. Glynne-Jones P, Hill M. 2013 Acoustofluidics 23: acoustic manipulation combined with other force fields. Lab Chip 13(6):1003–10 [PubMed: 23385298]
38. Drinkwater BW.2016Dynamic-field devices for the ultrasonic manipulation of microparticles. Lab Chip 16(13):2360–75 [PubMed: 27256513]
39. Destgeer G, Ha BH, Park J, Jung JH, Alazzam A, Sung HJ. 2015 Travelling surface acoustic waves microfluidics. Phys. Proc 70:34–37
40. Ding X, Lin SCS, Lapsley MI, Li S, Guo X, et al. 2012 Standing surface acoustic wave (SSAW) based multichannel cell sorting. Lab Chip 12(21):4228–31 [PubMed: 22992833]
41. Patel MV, Tovar AR, Lee AP. 2012 Lateral cavity acoustic transducer as an on-chip cell/particle microfluidic switch. Lab Chip 12(1):139–45 [PubMed: 22072298]
42. Hashmi A, Yu G, Reilly-Collette M, Heiman G, Xu J. 2012 Oscillating bubbles: a versatile tool for lab on a chip applications. Lab Chip 12(21):4216–27 [PubMed: 22864283]
43. Ahmed D, Chan CY, Lin SCS, Muddana HS, Nama N, Benkovic SJ, Huang TJ. 2013 Tunable, pulsatile chemical gradient generation via acoustically driven oscillating bubbles. Lab Chip 13(3):328–31 [PubMed: 23254861]
44. Thomas DH, Looney P, Steel R, Pelekasis N, McDicken WN, et al. 2009 Acoustic detection of microbubble resonance. Appl. Phys. Lett. 94(24):243902
45. Marmottant P, Hilgenfeldt S. 2004 A bubble-driven microfluidic transport element for bioengineering. PNAS 101(26):9523–27 [PubMed: 15210976]
46. Tovar AR, Patel MV, Lee AP. 2011 Lateral air cavities for microfluidic pumping with the use of acoustic energy. Microfluid. Nanofluid. 10(6):1269–78
47. Ren L, Nama N, McNeill JM, Soto F, Yan Z, et al. 2019 3D steerable, acoustically powered microswimmers for single-particle manipulation. Sci. Adv. 5(10):eaax3084 [PubMed: 31692692]
48. Huang PH, Nama N, Mao Z, Li P, Rufo J, et al. 2014 A reliable and programmable acoustofluidic pump powered by oscillating sharp-edge structures. Lab Chip 14(22):4319–23 [PubMed: 25188786]
49. Kaynak M, Ozcelik A, Nourhani A, Lammert PE, Crespi VH, Huang TJ. 2017 Acoustic actuation of bioinspired microswimmers. Lab Chip 17(3):395–400 [PubMed: 27991641]
50. Foresti D, Poulikakos D. 2014 Acoustophoretic contactless elevation, orbital transport and spinning of matter in air. Phys. Rev. Lett. 112(2):024301 [PubMed: 24484018]
51. Démoré CEM, Dahl PM, Yang Z, Glynne-Jones P, Melzer A, et al. 2014 Acoustic tractor beam. Phys. Rev. Lett. 112(17):174302 [PubMed: 24836252]
52. Marzo A, Seah SA, Drinkwater BW, Sahoo DR, Long B, Subramanian S. 2015 Holographic acoustic elements for manipulation of levitated objects. Nat. Commun. 6:8661 [PubMed: 26505138]
53. Cummer SA,Christensen J,Alù A.2016Controlling sound with acoustic metamaterials. Nat.Rev.Mater 1(3):16001
54. Naify CJ, Rohde CA, Martin TP, Nicholas M, Guild MD, Orris GJ. 2016 Generation of topologically diverse acoustic vortex beams using a compact metamaterial aperture. Appl. Phys. Lett. 108(22):223503

55. Melde K, Mark AG, Qiu T, Fischer P. 2016 Holograms for acoustics. Nature 537(7621):518–22 [PubMed: 27652563]
56. Li F, Cai F, Liu Z, Meng L, Qian M, et al. 2014 Phononic-crystal-based acoustic sieve for tunable manipulations of particles by a highly localized radiation force. Phys. Rev. Appl. 1(5):051001
57. Xie Y, Shen C, Wang W, Li J, Suo D, et al. 2016 Acoustic holographic rendering with two-dimensional metamaterial-based passive phased array. Sci. Rep. 6:35437 [PubMed: 27739472]
58. Ding X, Lin SCS, Kiraly B, Yue H, Li S, et al. 2012 On-chip manipulation of single microparticles, cells, and organisms using surface acoustic waves. PNAS 109(28):11105–9 [PubMed: 22733731]
59. Raeymaekers B, Pantea C, Sinha DN 2011 Manipulation of diamond nanoparticles using bulk acoustic waves. J. Appl. Phys 109(1):14317
60. Tian L, Martin N, Bassindale PG, Patil AJ, Li M, et al. 2016 Spontaneous assembly of chemically encoded two-dimensional coacervate droplet arrays by acoustic wave patterning. Nat. Commun. 7(1):13068 [PubMed: 27708286]
61. Marzo A, Drinkwater BW. 2019 Holographic acoustic tweezers. PNAS 116(1):84–89 [PubMed: 30559177]
62. Foresti D, Nabavi M, Klingauf M, Ferrari A, Poulikakos D. 2013 Acoustophoretic contactless transport and handling of matter in air. PNAS 110(31):12549–54 [PubMed: 23858454]
63. Vasileiou T, Foresti D, Bayram A, Poulikakos D, Ferrari A. 2016 Toward contactless biology: acoustophoretic DNA transfection. Sci. Rep. 6:20023 [PubMed: 26828312]
64. Zhou Q, Sariola V, Latifi K, Liimatainen V. 2016 Controlling the motion of multiple objects on a Chladni plate. Nat. Commun. 7:12764 [PubMed: 27611347]
65. Armstrong JPK, Maynard SA, Pence IJ, Franklin AC, Drinkwater BW, Stevens MM. 2019 Spatiotemporal quantification of acoustic cell patterning using Voronoï tessellation. Lab Chip 19(4):562–73 [PubMed: 30667009]
66. Ahmed S, Wang W, Mair LO, Fraleigh RD, Li S, et al. 2013 Steering acoustically propelled nanowire motors toward cells in a biologically compatible environment using magnetic fields. Langmuir 29(52):16113–18 [PubMed: 24345038]
67. Ren L, Yang S, Zhang P, Qu Z, Mao Z, et al. 2018 Standing surface acoustic wave (SSAW)-based fluorescence-activated cell sorter. Small 14(40):1801996
68. Zhang C, Huang KC, Rajwa B, Li J, Yang S, et al. 2017 Stimulated Raman scattering flow cytometry for label-free single-particle analysis. Optica 4(1):103–9
69. Piyasena ME, Suthanthiraraj PPA, Applegate RW, Goumas AM, Woods TA, et al. 2012 Multinode acoustic focusing for parallel flow cytometry. Anal. Chem. 84(4):1831–39 [PubMed: 22239072]
70. Destgeer G, Ha BH, Park J, Jung JH, Alazzam A, Sung HJ. 2015 Microchannel anechoic corner for size-selective separation and medium exchange via traveling surface acoustic waves. Anal. Chem. 87(9):4627–32 [PubMed: 25800052]
71. Garg N, Westerhof TM, Liu V, Liu R, Nelson EL, Lee AP. 2018 Whole-blood sorting, enrichment and *in situ* immunolabeling of cellular subsets using acoustic microstreaming. Microsyst. Nanoeng. 4:17085
72. Li S, Ma F, Bachman H, Cameron CE, Zeng X, Huang TJ. 2017 Acoustofluidic bacteria separation. J Micromech. Microeng. 27:15031
73. Wu M, Chen C, Wang Z, Bachman H, Ouyang Y, et al. 2019 Separating extracellular vesicles and lipoproteins via acoustofluidics. Lab Chip 19(7):1174–82 [PubMed: 30806400]
74. Gu Y, Chen C, Wang Z, Huang PH, Fu H, et al. 2019 Plastic-based acoustofluidic devices for high-throughput, biocompatible platelet separation. Lab Chip 19(3):394–402 [PubMed: 30631874]
75. Ma Z, Collins DJ, Ai Y. 2016 Detachable acoustofluidic system for particle separation via a traveling surface acoustic wave. Anal. Chem. 88(10):5316–23 [PubMed: 27086552]
76. Cushing K, Undvall E, Ceder Y, Lilja H, Laurell T. 2018 Reducing WBC background in cancer cell separation products by negative acoustic contrast particle immuno-acoustophoresis. Anal. Chim. Acta 1000:256–64 [PubMed: 29289318]
77. Faridi MA, Ramachandraiah H, Iranmanesh I, Grishenkov D, Wiklund M, Russom A. 2017 Micro-Bubble activated acoustic cell sorting. Biomed. Microdevices 19(2):23 [PubMed: 28374278]

78. Collins DJ, Neild A, Ai Y. 2016 Highly focused high-frequency travelling surface acoustic waves (SAW) for rapid single-particle sorting. Lab Chip 16(3):471–79 [PubMed: 26646200]
79. Schmid L, Weitz DA, Franke T. 2014 Sorting drops and cells with acoustics: acoustic microfluidic fluorescence-activated cell sorter. Lab Chip 14(19):3710–18 [PubMed: 25031157]
80. Chen K, Wu M, Guo F, Li P, Chan CY, et al. 2016 Rapid formation of size-controllable multicellular spheroids: via 3D acoustic tweezers. Lab Chip 16(14):2636–43 [PubMed: 27327102]
81. Collins DJ, Ma Z, Han J, Ai Y. 2017 Continuous micro-vortex-based nanoparticle manipulation via focused surface acoustic waves. Lab Chip 17(1):91–103
82. Hammarström B, Laurell T, Nilsson J. 2012 Seed particle-enabled acoustic trapping of bacteria and nanoparticles in continuous flow systems. Lab Chip 12(21):4296–304 [PubMed: 22955667]
83. Dorrestijn M, Bietsch A, Açikalin T, Raman A, Hegner M, et al. 2007 Chladni figures revisited based on nanomechanics. Phys. Rev. Lett. 98(2):026102 [PubMed: 17358621]
84. Weiwei C, He M, Zhang H, Yang Y, Xuexin D. 2016 Bulk acoustic wave resonator integrated microfluidics for rapid and high efficience fluids mixing and bioparticle trapping In 2016 IEEE International Ultrasonics Symposium, pp. 1–3. New York: IEEE
85. Destgeer G,Cho H,Ha BH,Jung JH,Park J,Sung HJ.2016Acoustofluidic particle manipulation inside a sessile droplet: four distinct regimes of particle concentration. Lab Chip 16(4):660–67 [PubMed: 26755271]
86. Ahmed H, Rezk AR, Richardson JJ, Macreadie LK, Babarao R, et al. 2019 Acoustomicrofluidic assembly of oriented and simultaneously activated metal-organic frameworks. Nat. Commun. 10:2282 [PubMed: 31123252]
87. Zhang J, Yang S, Chen C, Hartman JH, Huang PH, et al. 2019 Surface acoustic waves enable rotational manipulation of *Caenorhabditis elegans.* Lab Chip 19(6):984–92 [PubMed: 30768117]
88. Tian Z, Yang S, Huang PH, Wang Z, Zhang P, et al. 2019 Wave number-spiral acoustic tweezers for dynamic and reconfigurable manipulation of particles and cells. Sci. Adv. 5(5):eaau6062 [PubMed: 31172021]
89. Collins DJ, Morahan B, Garcia-Bustos J, Doerig C, Plebanski M, Neild A. 2015 Two-dimensional single-cell patterning with one cell per well driven by surface acoustic waves. Nat. Commun. 6:8686 [PubMed: 26522429]
90. Schmid L, Wixforth A, Weitz DA, Franke T. 2012 Novel surface acoustic wave (SAW)-driven closed PDMS flow chamber. Microfluid. Nanofluid. 12(1–4):229–35
91. Huang PH, Ren L, Nama N, Li S, Li P, et al. 2015 An acoustofluidic sputum liquefier. Lab Chip 15(15):3125–31 [PubMed: 26082346]
92. Guttenberg Z, Müller H, Habermüller H, Geisbauer A, Pipper J, et al. 2005 Planar chip device for PCR and hybridization with surface acoustic wave pump. Lab Chip 5(3):308–17 [PubMed: 15726207]
93. Reboud J, Bourquin Y, Wilson R, Pall GS, Jiwaji M, et al. 2012 Shaping acoustic fields as a toolset for microfluidic manipulations in diagnostic technologies. PNAS 109(38):15162–67 [PubMed: 22949692]
94. Rezk AR, Ramesan S, Yeo LY. 2018 Plug-and-actuate on demand: multimodal individual addressability of microarray plates using modular hybrid acoustic wave technology. Lab Chip 18(3):406–11 [PubMed: 29231220]
95. Zhang SP, Lata J, Chen C, Mai J, Guo F, et al. 2018 Digital acoustofluidics enables contactless and programmable liquid handling. Nat. Commun. 9:2928 [PubMed: 30050088]
96. Jung JH, Destgeer G, Park J, Ahmed H, Park K, Sung HJ. 2017 On-demand droplet capture and release using microwell-assisted surface acoustic waves. Anal. Chem. 89(4):2211–15 [PubMed: 28192923]
97. Collins DJ, Alan T, Helmerson K, Neild A. 2013 Surface acoustic waves for on-demand production of picoliter droplets and particle encapsulation. Lab Chip 13(16):3225–31 [PubMed: 23784263]
98. Fornell A, Garofalo F, Nilsson J, Bruus H, Tenje M. 2018 Intra-droplet acoustic particle focusing: simulations and experimental observations. Microfluid. Nanofluid. 22(7):75
99. Jung JH, Destgeer G, Ha B, Park J, Sung HJ. 2016 On-demand droplet splitting using surface acoustic waves. Lab Chip 16(17):3235–43 [PubMed: 27435869]

100. Demirci U. 2006 Acoustic picoliter droplets for emerging applications in semiconductor industry and biotechnology. J. Microelectromech. Syst. 15(4):957–66
101. Lee CY, Yu H, Kim ES. 2006 Acoustic ejector with novel lens employing air-reflectors. In 19th IEEE International Conference on Micro Electro Mechanical Systems, pp. 170–73. New York: IEEE
102. Foresti D, Kroll KT, Amissah R, Sillani F, Homan KA, et al. 2018 Acoustophoretic printing. Sci. Adv. 4(8):eaat1659 [PubMed: 30182058]
103. Heron SR, Wilson R, Shaffer SA, Goodlett DR, Cooper JM. 2010 Surface acoustic wave nebulization of peptides as a microfluidic interface for mass spectrometry. Anal. Chem. 82(10):3985–89 [PubMed: 20364823]
104. Miansari M, Friend JR. 2016 Acoustic nanofluidics via room-temperature lithium niobate bonding: a platform for actuation and manipulation of nanoconfined fluids and particles. Adv. Funct. Mater. 26(43):7861–72
105. Rezk AR, Manor O, Friend JR, Yeo LY. 2012 Unique fingering instabilities and soliton-like wave propagation in thin acoustowetting films. Nat. Commun. 3:1167 [PubMed: 23132017]
106. Coussios CC, Farny CH, ter Haar G, Roy RA. 2007 Role of acoustic cavitation in the delivery and monitoring of cancer treatment by high-intensity focused ultrasound (HIFU). Int.J.Hyperth 23(2):105–20
107. Izadifar Z, Babyn P, Chapman D. 2019 Ultrasound cavitation/microbubble detection and medical applications. J. Med. Biol. Eng. 39(3):259–76
108. Fan Z, Liu H, Mayer M, Deng CX. 2012 Spatiotemporally controlled single cell sonoporation. PNAS 109(41):16486–91 [PubMed: 23012425]
109. Neumann F, Madaboosi N, Hernández-Neuta I, Salas J, Ahlford A, et al. 2018 QCM mass underestimation in molecular biotechnology: proximity ligation assay for norovirus detection as a case study. Sens. Actuators B Chem. 273:742–50
110. Zhang Y, Luo J, Flewitt AJ, Cai Z, Zhao X. 2018 Film bulk acoustic resonators (FBARs) as biosensors: a review. Biosens. Bioelectron. 116:1–15 [PubMed: 29852471]
111. Thomas S, Cole M, Villa-López FH, Gardner JW. 2016 High frequency surface acoustic wave resonator-based sensor for particulate matter detection. Sens. Actuators A Phys. 244:138–45
112. Rana L, Gupta R, Tomar M, Gupta V. 2018 Highly sensitive Love wave acoustic biosensor for uric acid. Sens. Actuators B Chem. 261:169–77
113. Hartono D, Liu Y, Tan PL, Then XYS, Yung LYL, Lim KM. 2011 On-chip measurements of cell compressibility via acoustic radiation. Lab Chip 11(23):4072–80 [PubMed: 22020269]
114. Baasch T, Reichert P, Lakämper S, Vertti-Quintero N, Hack G, et al. 2018 Acoustic compressibility of *Caenorhabditis elegans*. Biophys. J. 115(9):1817–25 [PubMed: 30314654]
115. Cermak N, Olcum S, Delgado FF, Wasserman SC, Payer KR, et al. 2016 High-throughput measurement of single-cell growth rates using serial microfluidic mass sensor arrays. Nat.Biotechnol. 34(10):1052–59 [PubMed: 27598230]
116. Sitters G, Kamsma D, Thalhammer G, Ritsch-Marte M, Peterman EJG, Wuite GJL. 2014 Acoustic force spectroscopy. Nat. Methods 12(1):47–50 [PubMed: 25419961]
117. Guo F, Zhou W, Li P, Mao Z, Yennawar NH, et al. 2015 Precise manipulation and patterning of protein crystals for macromolecular crystallography using surface acoustic waves. Small 11(23):2733–37 [PubMed: 25641793]
118. Bryan AK, Hecht VC, Shen W, Payer K, Grover WH, Manalis SR. 2014 Measuring single cell mass, volume, and density with dual suspended microchannel resonators. Lab Chip 14(3):569–76 [PubMed: 24296901]
119. Bouyer C, Chen P, Güven S, Demirtaş TT, Nieland TJF, et al. 2016 A bio-acoustic levitational (BAL) assembly method for engineering of multilayered, 3D brain-like constructs, using human embryonic stem cell derived neuro-progenitors. Adv. Mater. 28(1):161–67 [PubMed: 26554659]
120. Kang B, Shin J, Park HJ, Rhyou C, Kang D, et al. 2018 High-resolution acoustophoretic 3D cell patterning to construct functional collateral cylindroids for ischemia therapy. Nat. Commun. 9:5402 [PubMed: 30573732]

121. Zhou W, Wang J, Wang K, Huang B, Niu L, et al. 2017 Ultrasound neuro-modulation chip: activation of sensory neurons in *Caenorhabditis elegans* by surface acoustic waves. Lab Chip 17(10):1725–31 [PubMed: 28447086]
122. Ibsen S, Tong A, Schutt C, Esener S, Chalasani SH. 2015 Sonogenetics is a non-invasive approach to activating neurons in *Caenorhabditis elegans*. Nat. Commun. 6:8264 [PubMed: 26372413]
123. Yang Z, Cole KLH, Qiu Y, Somorjai IML, Wijesinghe P, et al. 2019 Light sheet microscopy with acoustic sample confinement. Nat. Commun. 10:669 [PubMed: 30737391]
124. Antfolk M, Magnusson C, Augustsson P, Lilja H, Laurell T. 2015 Acoustofluidic, label-free separation and simultaneous concentration of rare tumor cells from white blood cells. Anal. Chem. 87(18):9322–28 [PubMed: 26309066]
125. Travagliati M, Shilton RJ, Pagliazzi M, Tonazzini I, Beltram F, Cecchini M. 2014 Acoustofluidics and whole-blood manipulation in surface acoustic wave counterflow devices. Anal. Chem. 86(21):10633–38 [PubMed: 25260018]
126. Taller D, Richards K, Slouka Z, Senapati S, Hill R, et al. 2015 On-chip surface acoustic wave lysis and ion-exchange nanomembrane detection of exosomal RNA for pancreatic cancer study and diagnosis. Lab Chip 15(7):1656–66 [PubMed: 25690152]
127. Galanzha EI, Viegas MG, Malinsky TI, Melerzanov AV, Juratli MA, et al. 2016 *In vivo* acoustic and photoacoustic focusing of circulating cells. Sci. Rep. 6(1):21531 [PubMed: 26979811]
128. Collins DJ, Ma Z, Ai Y. 2016 Highly localized acoustic streaming and size-selective submicrometer particle concentration using high frequency microscale focused acoustic fields. Anal.Chem. 88(10):5513–22 [PubMed: 27102956]
129. Whitehill JD, Gralinski I, Joiner D, Neild A. 2012 Nanoparticle manipulation within a microscale acoustofluidic droplet. J. Nanopart. Res 14(11):1223
130. Mao Z, Li P, Wu M, Bachman H, Mesyngier N, et al. 2017 Enriching nanoparticles via acoustofluidics. ACS Nano 11(1):603–12 [PubMed: 28068078]
131. Sehgal P, Kirby BJ. 2017 Separation of 300 and 100 nm particles in Fabry-Perot acoustofluidic resonators. Anal. Chem. 89(22):12192–200 [PubMed: 29039191]
132. Wu M, Mao Z, Chen K, Bachman H, Chen Y, et al. 2017 Acoustic separation of nanoparticles in continuous flow. Adv. Funct. Mater. 27(14):1606039 [PubMed: 29104525]
133. Tang SY, Qiao R, Lin Y, Li Y, Zhao Q, et al. 2019 Functional liquid metal nanoparticles produced by liquid-based nebulization. Adv. Mater. Technol. 4(2):1800420
134. Smorodin T, Beierlein U, Ebbecke J, Wixforth A. 2005 Surface-acoustic-wave-enhanced alignment of thiolated carbon nanotubes on gold electrodes. Small 1(12):1188–90 [PubMed: 17193416]
135. Kang JH,Miettinen TP,Chen L,Olcum S,Katsikis G,et al.2019Noninvasive monitoring of single-cell mechanics by acoustic scattering. Nat. Methods 16(3):263–69 [PubMed: 30742041]
136. Olcum S, Cermak N, Wasserman SC, Manalis SR. 2015 High-speed multiple-mode mass-sensing resolves dynamic nanoscale mass distributions. Nat. Commun. 6:7070 [PubMed: 25963304]
137. Lee J, Shen W, Payer K, Burg TP, Manalis SR. 2010 Toward attogram mass measurements in solution with suspended nanochannel resonators. Nano Lett. 10(7):2537–42 [PubMed: 20527897]
138. Burg TP, Manalis SR. 2003 Suspended microchannel resonators for biomolecular detection. Appl. Phys. Lett. 83(13):2698–700
139. Wang H, Liu Z, Shin DM, Chen ZG, Cho Y, et al. 2019 A continuous-flow acoustofluidic cytometer for single-cell mechanotyping. Lab Chip 19(3):387–93 [PubMed: 30648172]
140. Strohm EM, Gnyawali V, Sebastian JA, Ngunjiri R, Moore MJ, et al. 2019 Sizing biological cells using a microfluidic acoustic flow cytometer. Sci. Rep. 9:4775 [PubMed: 30886171]
141. Hwang JY, Kim J, Park JM, Lee C, Jung H, et al. 2016 Cell deformation by single-beam acoustic trapping: a promising tool for measurements of cell mechanics. Sci. Rep. 6:27238 [PubMed: 27273365]
142. Chen F, Lin L, Zhang J, He Z, Uchiyama K, Lin JM. 2016 Single-cell analysis using drop-on-demand inkjet printing and probe electrospray ionization mass spectrometry. Anal. Chem. 88(8):4354–60 [PubMed: 27015013]

143. Guo F, Li P, French JB, Mao Z, Zhao H, et al. 2015 Controlling cell-cell interactions using surface acoustic waves. PNAS 112(1):43–48 [PubMed: 25535339]

144. Guo F, Mao Z, Chen Y, Xie Z, Lata JP, et al. 2016 Three-dimensional manipulation of single cells using surface acoustic waves. PNAS 113(6):1522–27 [PubMed: 26811444]

145. Riaud A, Baudoin M, Bou Matar O, Becerra L, Thomas JL. 2017 Selective manipulation of microscopic particles with precursor swirling Rayleigh waves. Phys. Rev. Appl. 7(2):024007

146. Demirci U, Montesano G. 2007 Single cell epitaxy by acoustic picolitre droplets. Lab Chip 7(9):1139–45 [PubMed: 17713612]

147. Trinh EH. 1985 Compact acoustic levitation device for studies in fluid dynamics and material science in the laboratory and microgravity. Rev. Sci. Instrum. 56(11):2059–65

148. Kwon JW, Yu H, Zou Q, Kim ES. 2006 Directional droplet ejection by nozzleless acoustic ejectors built on ZnO and PZT. J. Micromech. Microeng 16(12):2697–704

149. Sesen M, Devendran C, Malikides S, Alan T, Neild A. 2017 Surface acoustic wave enabled pipette on a chip. Lab Chip 17(3):438–47 [PubMed: 27995242]

150. Langelier SM, Chang DS, Zeitoun RI, Burns MA. 2009 Acoustically driven programmable liquid motion using resonance cavities. PNAS 106(31):12617–22 [PubMed: 19620719]

151. Zhao S, He W, Ma Z, Liu P, Huang PH, et al. 2019 On-chip stool liquefaction via acoustofluidics. Lab Chip 19(6):941–47 [PubMed: 30702741]

152. Petersson K, Jakobsson O, Ohlsson P, Augustsson P, Scheding S, et al. 2018 Acoustofluidic hematocrit determination. Anal. Chim. Acta 1000:199–204 [PubMed: 29289309]

153. Wu M, Huang PH, Zhang R, Mao Z, Chen C, et al. 2018 Circulating tumor cell phenotyping via high-throughput acoustic separation. Small 14(32):1870145

154. Liu H, Ao Z, Cai B, Shu X, Chen K, et al. 2018 Size-amplified acoustofluidic separation of circulating tumor cells with removable microbeads. Nano Futures 2(2):25004

155. Nguyen TD, Tran VT, Fu YQ, Du H. 2018 Patterning and manipulating microparticles into a three-dimensional matrix using standing surface acoustic waves. Appl. Phys. Lett. 112(21):213507

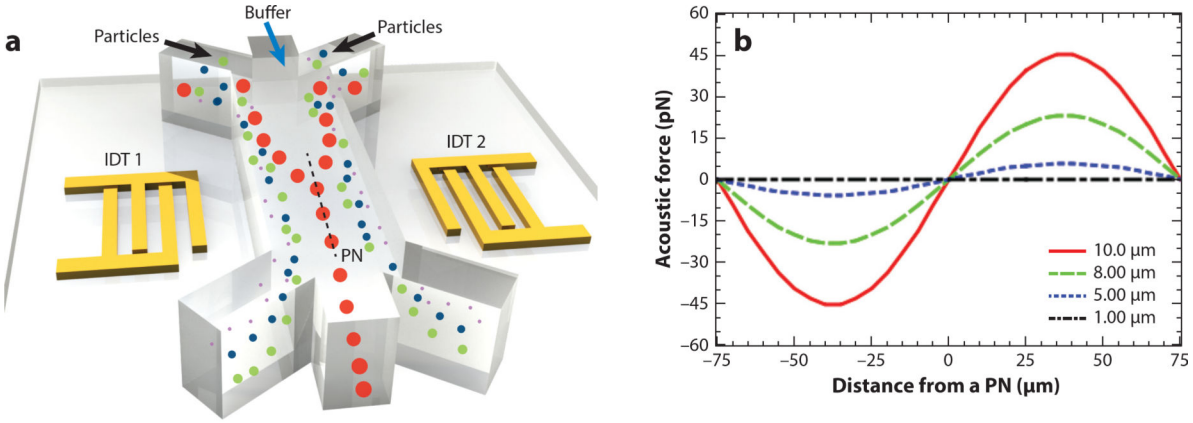


**Figure 1.**

Effect of primary acoustic radiation force on various particles. (*a*) Radio frequency signals applied to two oppositely positioned interdigitated transducers (IDTs) generate a standing surface acoustic wave (SAW) field. When a mixture of particles with the same physical properties but different sizes is introduced into the standing SAW field, the primary acoustic radiation force scales with the volume of the particles. Larger particles experience a larger force so they are pulled toward the pressure node (PN) quicker than smaller particles. If a single PN exists inside a microchannel, as depicted here, larger particles in the mixture injected from the side inlets migrate to the PN faster so that they eventually exit the channel from the middle outlet while the rest of the particles go to the side outlets. (*b*) The calculated primary acoustic radiation force on 10-, 8-, 5-, and 1-μm polystyrene particles for an acoustic wavelength of 300 μm and an acoustic pressure of 0.2 MPa in deionized (DI) water. $\beta_f$ (fluid compressibility), $\rho_f$ (fluid density), $\beta_p$ (particle compressibility), and $\rho_p$(particledensity) are taken as $4.6\times10^{-10}$ $Pa^{-1}$, 1,000 kg· $m^{-3}$, 2.16 $\times10^{-10}Pa^{-1}$ and 1,050 kg· $m^{-3}$, respectively, for polystyrene particles and DI water.

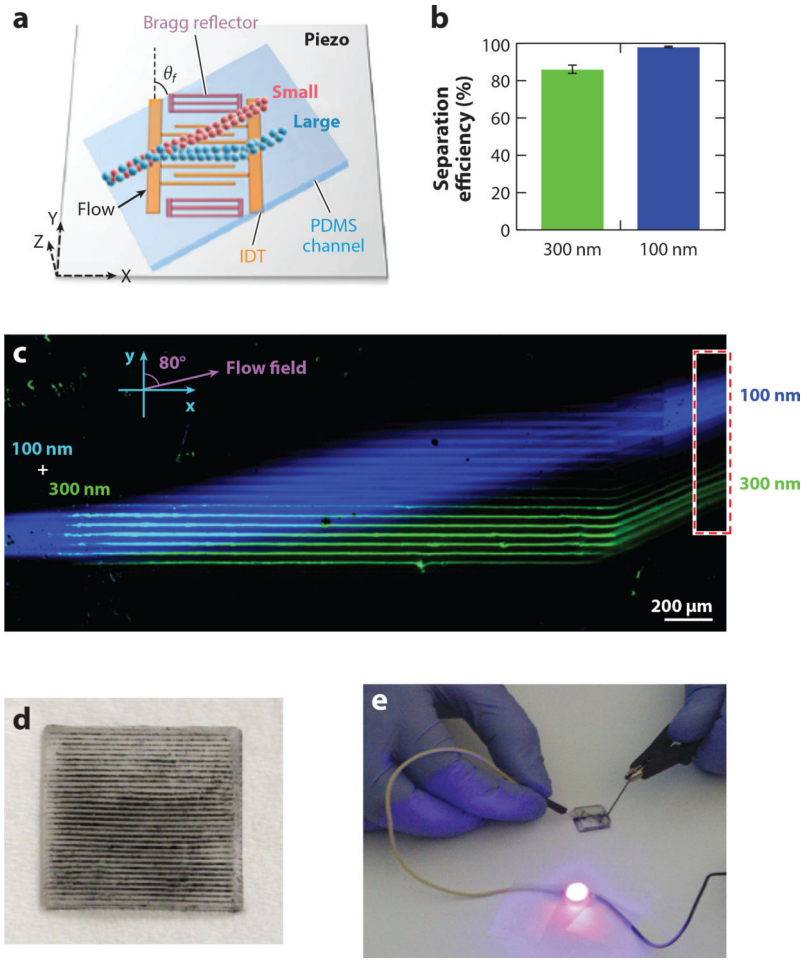


**Figure 2.**

(*a*) Schematic of a surface acoustic wave (SAW)-based nanoparticle separation chip. (*b*) Separation efficiency and (*c*) fluorescent image of nanoparticle separation in the SAW separation device, respectively. (*d*,*e*) Demonstration of horizontal nanoparticle patterning and LED lighting using a simple nanoparticle patterned circuit. Panels *a*–*c* are adapted with permission from Reference 131. Copyright 2017, American Chemical Society. Panels *d* and *e* are adapted with permission from Reference 20. Copyright 2017, IOP. Abbreviations: IDT, interdigitated transducer; PDMS, polydimethylsiloxane.

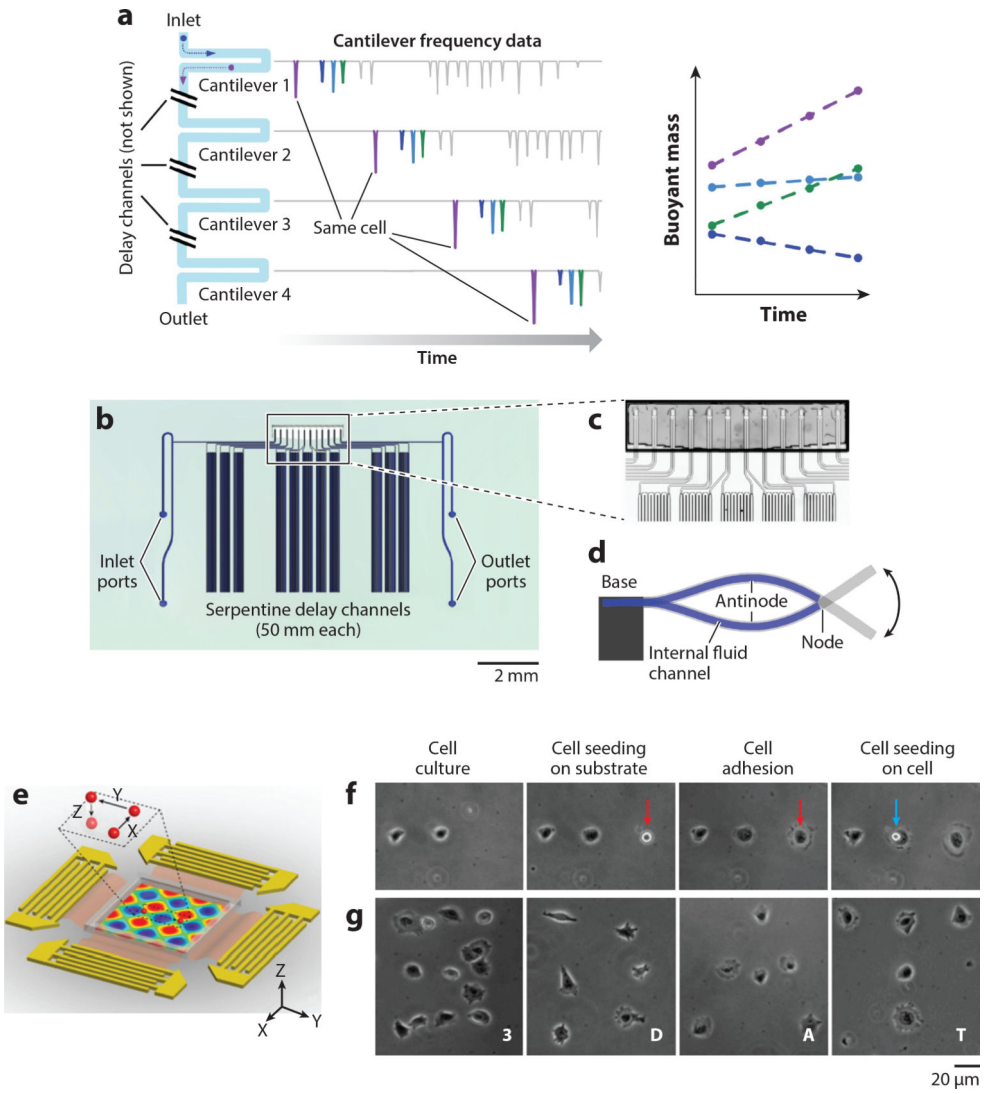


**Figure 3.**

Single-cell analysis via acoustic microfluidics. (*a–d*) Design and implementation of the serial suspended microchannel resonator (SMR) array. (*a*) Schematic working mechanism of serial SMR array. The mass accumulation rate of single cells flowing through can be monitored with respect to time. (*b*) Device layout and (*c*) microscopic picture of the serial SMR array. The serpentine channels create a time delay for cells to grow. (*d*) Schematic side view of a suspended microchannel vibrating in the second bending mode. (*e–g*)3D acoustic tweezers. (*e*) Schematic device layout. A particle can be dynamically programmed to move in 3D space in the microchamber. (*f*) Single-cell printing. (*g*) Creating arbitrary cell adhesion patterns via 3D acoustic tweezers. Panels *a–d* adapted with permission from Reference 115. Copyright 2016, Springer Nature. Panels *e–g* adapted with permission from Reference 144 and the National Academy of Sciences.

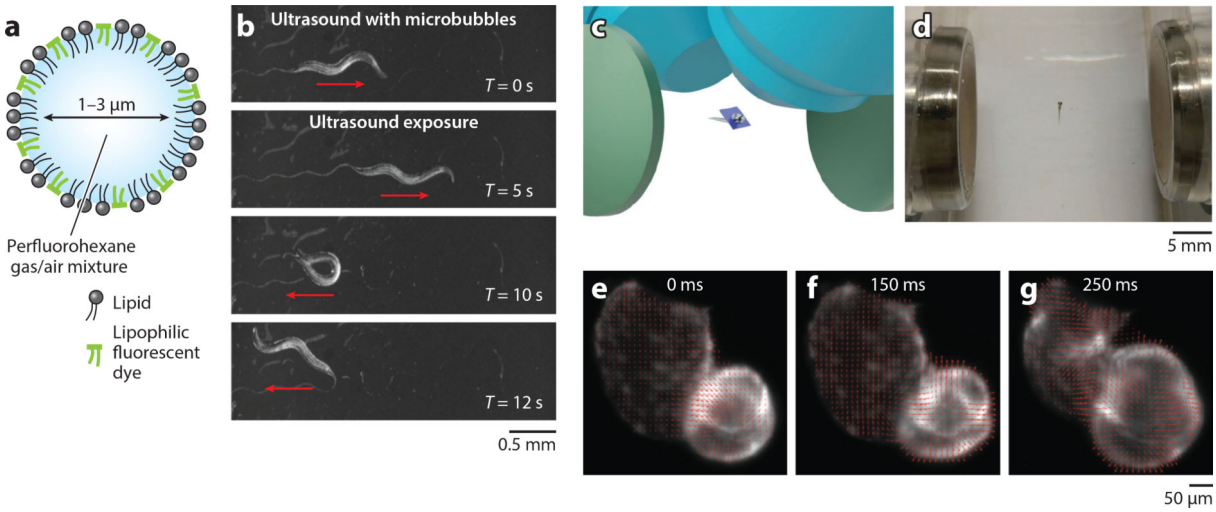


**Figure 4.**

Model organism manipulation via acoustic microfluidics. (*a*,*b*) Sonogenetics for on-demand neuron activation and behavioral modulation of *Caenorhabditis elegans.* (*a*) Schematic of an engineered microbubble for ultrasound actuation. (*b*) *C. elegans* exhibit reversals and omega bends upon acoustic stimulation with microbubbles. (*c*–*g*) Light-sheet microscopy with acoustic sample confinement. (*c*) Schematic showing the immersed acoustic transducers (*green*), trapped model organism (zebrafish embryo in center), scanning light sheet *(dark blue plane*), and objectives (*light blue*). (*d*) A zebrafish larva 5 days postfertilization is trapped and confined in free space using acoustic gradient force. (*e*–*g*) The cardiac cycle of the trapped larva is profiled using the velocity vector plot with optical flow analysis: (*e*) contraction of the ventricle, ( *f* ) relaxation of the ventricle, (*g*) contraction of the atrium. Panels *a* and *b* are adapted with permission from Reference 122 and panels *c*–*g* from Reference 123 under the terms of the Creative Commons Attribution (CC BY) License, http://creativecommons.org/licenses/by/4.0.

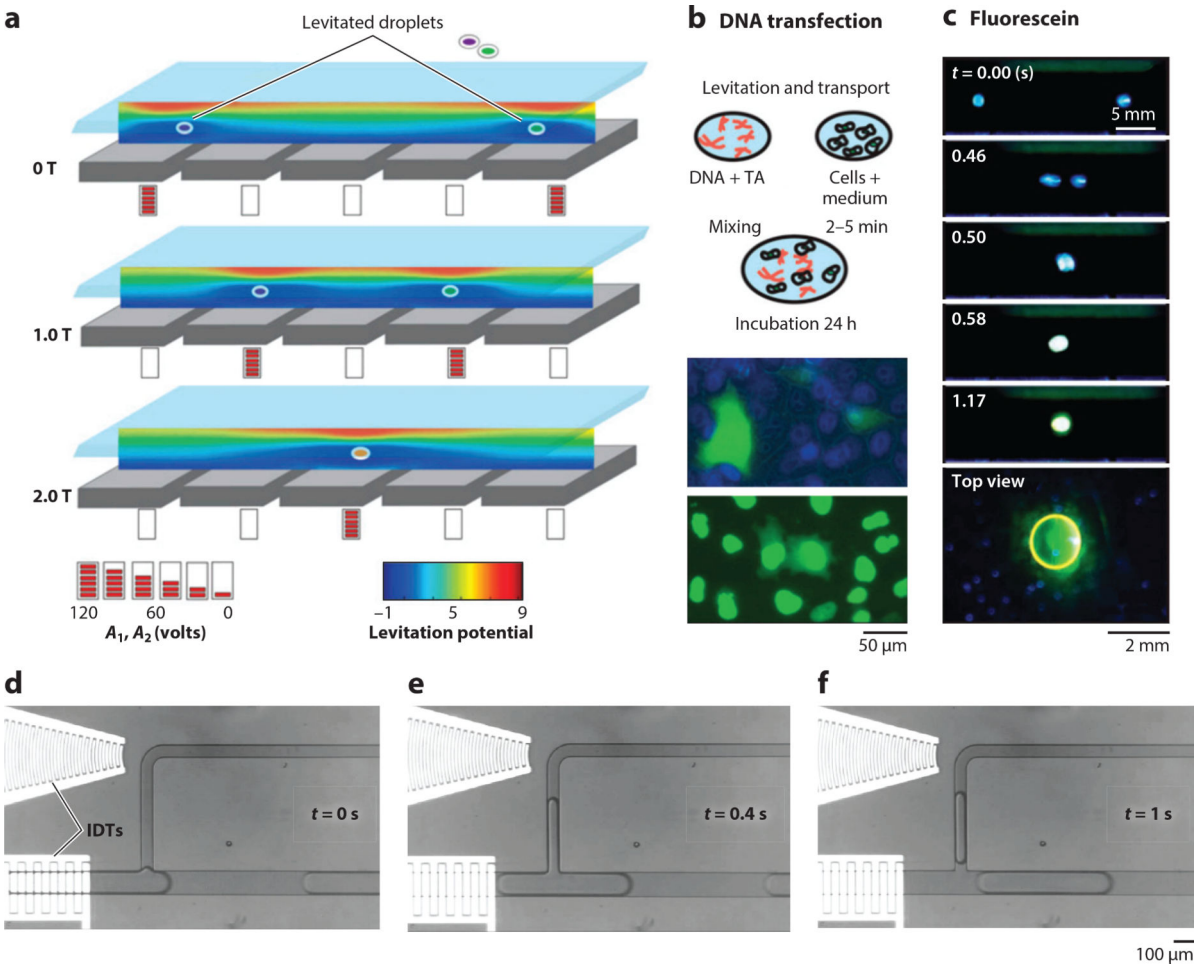


**Figure 5.**

Fluid actuation via acoustic microfluidics. (*a–c*) Contactless liquid handling via acoustic levitation. (*a*) Controlled translation and merging of two droplets in air by spatiotemporally varying the levitation potential inside a five Langevin piezoelectric transducer (LPT). The blue region indicates the levitation nodes. (*b*) Schematic contactless DNA transfection process and experimental images of the transfected cells in 96-well plate. (*c*) Droplet merging experiment demonstrating the switching of photochemical fluorescein under different pH values. Panels *a–c* adapted with permission from Reference 62 and the National Academy of Sciences. (*d–f*) Time-lapse images of droplet pipetting using surface acoustic waves. Panels *d–f* adapted with permission from Reference 149. Copyright 2016, Royal Society of Chemistry. Abbreviations: IDT, interdigitated transducer; TA, transfection agent.

**Table 1**

Summary of the manipulation of biosamples via acoustic microfluidics

| Types | Subtypes | Manipulation | Mechanism |
|---|---|---|---|
| Macro-molecules | Sensitive bioreagents and bioanalytes, e.g., antibodies, enzymes | Contact-free liquid handling | Acoustic levitation (62)<br>Acoustic streaming (95) |
| | | Acoustic droplet ejection<br>Acoustophoretic printing | Traveling SAW (100)<br>Traveling/standing BAW (102) |
| | | Patterning (with coacervation) | Standing BAW (60) |
| | | Atomization | Traveling SAW (103) |
| | Protein crystals | Trapping for crystallography | Standing SAW (117) |
| Cell lines | Hela, MCF-7, HEK293, RBCs, WBCs, bacteria, etc. | Patterning, translation, separation, sorting, orientational control, lysis | Standing/traveling SAW/BAW (3,89)<br>Acoustic streaming |
| | | Rotation for imaging | Acoustic streaming (18) |
| | | Biophysical measurements, e.g., mass, density, stiffness, compressibility, acoustic impedance, adhesión forces | Standing BAW (2, 113)<br>Acoustic resonance (115, 116, 118) |
| | | Single-cell cargo delivery via sonoporation | Focused traveling BAW (108) |
| Tissue engineering | Spheroids | Clustering, patterning | Standing SAW (80) |
| | Neuroprogenitor stem cell network | 3D patterning for in-gel cultivation | Standing BAW (119) |
| | HUVEC/hADSC mixture | 3D patterning for in-gel cultivation | Standing BAW (120) |
| Model organisms | *C. elegans* larvae | Rotation for imaging | Acoustic streaming (18)<br>SAW (87) |
| | | Translation, orientation | Standing SAW (58) |
| | | Acousto-mechanical stimuli, sonogenetics | Traveling SAW (121)<br>Focused traveling BAW (122) |
| | | Compressibility measurement | Standing BAW (114) |
| | *D. rerio* embryo, *C. intestinalis* embryo, *B. lanceolatum* embryo | Trapping for light sheet microscopy | BAW gradient force trap (123) |
| Patient samples | Whole blood (targets: exosomes, lipo-proteins, platelets, circulating tumor cells, bacteria, etc.) | Separation | Standing SAW/BAW (3,124)<br>Acoustic streaming (71) |
| | | Pumping, mixing | Traveling SAW (125)<br>Acoustic streaming (91) |
| | | Lysis, thermocycling for diagnostics | Acoustic streaming (126)<br>Acousto-thermal effect (93) |
| | In vivo manipulation of RBCs in vessel | Trapping, deflection | Traveling BAW (127) |
| | Sputum | Liquefaction | Acoustic streaming (18) |
| | Stool | Liquefaction | Acoustic streaming (6) |

Abbreviations: BAW, bulk acoustic wave; hADSC, human adipose-derived stem cell; HUVEC, human umbilical vein endothelial cell; RBC, red blood cell; SAW, surface acoustic wave; WBC, white blood cell.